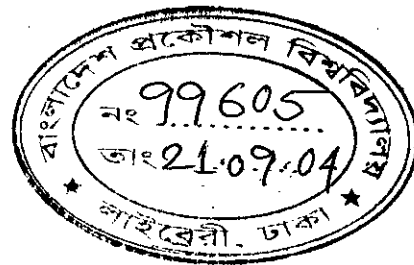


**An Experimental Investigation of Wind Effect on Rectangular Cylinders with Rounded  
Corners**

by  
**Gazi Md. Golam Farok**

A Thesis  
Submitted to the Department of Mechanical Engineering in Partial fulfillment  
of the Requirements for the Degree of  
**MASTER OF SCIENCE IN MECHANICAL ENGINEERING.**



#99605#

**BANGLADESH UNIVERSITY OF ENGINEERING AND TECHNOLOGY, DHAKA,  
BANGLADESH**

**AUGUST 2004**

**BANGLADESH UNIVERSITY OF ENGINEERING AND TECHNOLOGY, DHAKA  
DEPARTMENT OF MECHANICAL ENGINEERING**

**Certificate of Thesis Work**

The Thesis titled "**An Experimental Investigation of Wind Effect on Rectangular Cylinder with Rounded Corners**" submitted by **Gazi Md. Golam Farok**, Roll No. 100110014P, Session: October 2001 to October 2003 has been accepted as satisfactory in partial fulfillment of the requirement of the degree of Master of Science in Mechanical Engineering on August, 2004.

## RECOMMENDATION OF THE BOARD OF EXAMINERS

The Board of Examiners hereby recommends to the Department of Mechanical Engineering, Bangladesh University of Engineering and Technology (BUET), Dhaka, the acceptance of the Thesis on "**An Experimental Investigation of Wind Effect on rectangular Cylinder with Rounded Corners**", submitted by Gazi Md. Golam Farok, in partial fulfillment of the requirement for the degree of Master of Science in Mechanical Engineering.



Dr. Amalesh Chandra Mandal  
Professor  
Department of Mechanical Engineering  
BUET, Dhaka.

Chairman



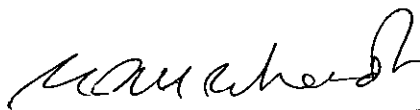
Dr. Dipak Kanti Das  
Professor  
Department of Mechanical Engineering  
BUET, Dhaka.

Member



Dr. Md. Quamrul Islam  
Professor and Head  
Department of Mechanical Engineering  
BUET, Dhaka.

Member  
(Ex-Officio)



Dr. Reaz Hasan Khondokar  
Professor  
Department of Naval Architecture  
and Marine Engineering  
BUET, Dhaka.

Member  
(External)

## CANDIDATE'S DECLARATION

It is hereby declared that this thesis or any part of it has not been submitted elsewhere for the award of any degree or diploma.



---

Signature of the Candidate

**Gazi Md. Golam Farok**

---

Name of the Candidate

**DEDICATED TO  
MY  
LATE FATHER**

## ACKNOWLEDGEMENTS

The author wishes to express his sincere appreciation to Professor Dr. Amalesh Chandra Mandal of Mechanical Engineering Department, Bangladesh University of Engineering and Technology (BUET), Dhaka, Bangladesh for his guidance, invaluable suggestions and constructive criticism throughout this investigation and for painstakingly reading the manuscript and suggesting its improvement. His encouragement, patience and careful supervisions are gratefully acknowledged.

The author is also indebted to Engr. Kazi Md. Sheesh, Ex-Chief Engineer, Dhaka WASA and Dr. Md. Ashraf Islam, Associate Professor of Mechanical Engineering Department, BUET for their stimulating discussions and numerous suggestions on various aspect of this problem. Further his sincere felicitation and gratitude are due to Professor Dr. Md. Quamrul Islam of Mechanical Engineering Department, BUET for taking care of him during the progress of research work from time to time.

Special thanks are due to Professor Dr. Md. Abdur Rashid Sarkar of Mechanical Engineering Department, BUET and Engr. Mohammad Shahjahan, S.E & P.D. of Dhaka WASA for their constant encouragement and invaluable advice during preparation of this thesis.

The author gratefully acknowledges the financial assistance given by Bangladesh University of Engineering and Technology (BUET), Dhaka. The author is obliged to the authority of Dhaka WASA for granting leave and partly relieving the office duties until this work was finished.

Sincere thanks are offered to the staff of the Machine Shop, Carpentry Shop, Welding Shop, Sheet Metal Shop, Pattern Shop and technicians of Fluid Mechanics Laboratory of Mechanical Engineering Department of BUET, Dhaka for their kind co-operation in constructing, fabricating and assembling different parts and components of the experimental set-up.

Finally, the author will be forever grateful for the patient understanding shown by his beloved wife, Salma and daughter, Fahmy during the preparation of this thesis.

## ABSTRACT

An experimental investigation of the static pressure distribution on the square and rectangular cylinders with rounded corners is conducted. The study incorporates both the single cylinder and the group consisting of two cylinders. The test is conducted in open circuit wind tunnel at a Reynolds number of  $2.87 \times 10^4$  and  $4.30 \times 10^4$  based on the side dimension across the flow with uniform flow of velocity 14.2 m/s.

First of all, the study is conducted on a single cylinder with various nose radius and side dimensions at zero angle of attack. The three different dimensionless nose radius are considered in the study with a view to observing the effect of the nose radius on the static pressure distribution.

Then a group of cylinder is taken into consideration for the study. Each group consists of two cylinders one is front and the other is rear which are kept along the flow direction. The static pressure distribution is done on each cylinders in the group varying the inter spacing between the front and rear cylinders. At a particular dimensionless nose radius the study is done on the group.

The drag coefficient which is essential to find wind load is determined from the static pressure distributions by the numerical integration method. It is observed from the results that the drag coefficient value depends on the nose radius significantly. With the rounded nose on the cylinder the drag reduces remarkably compared to that on the sharp edged cylinders, however, with further increase of nose radius, drag does not change that much. The effect of inter space is prominent observed on the inter space in the group. An empirical relation of drag coefficient as a function of dimensionless nose radius is presented in order to calculate the drag coefficient on a freestanding building.

## CONTENTS

	Page no
Certificate of Research	ii
Recommendation of the Board of Examiners	iii
Acknowledgements	vi
Abstract	vii
Contents	viii
List of Figures	x
List of Symbols	xii
Chapter 1: Introduction	1
1.1 Background	1
1.2 Nature of the Wind	2
1.2.1 Wind Velocity	2
1.2.2 Generation of Wind	3
1.2.3 Forces Governing Wind	4
1.2.4 Wind Loading on Structures	5
1.3 Importance of the study	6
1.4 Why model study	8
1.5 Aim of the Study	9
1.6 Scope of the Study	10
Chapter 2: Review of Literatures	11
Chapter 3: Experimental Set-up	20
3.1 Measurement of Wind Characteristics	20
3.2 Types of Wind Tunnel	22
3.3 Specification of the Wind Tunnel	22
3.4 Test Section	23
3.5 Constructional Details of Cylinder	24
3.6 Test of the Single Cylinder	25
3.7 Test of the cylinder in Group	26



Chapter 4: Mathematical Model	27
4.1 Calculation Procedure	27
4.2 Sample Calculation	30
Chapter 5: Results and Discussions	32
5.1 Single Cylinder	32
5.1.1 Static Pressure Coefficient	32
5.1.2 Drag Coefficients	34
5.2 Cylinders in a Group	35
5.2.1 Static Pressure Coefficients	35
5.2.2 Drag Coefficients	38
Chapter 6: Conclusions and Recommendations	41
6.1 Conclusions	41
6.2 Recommendations	42
References	43
Figures	49
Table-1	21

## LIST OF FIGURES

### Figures:

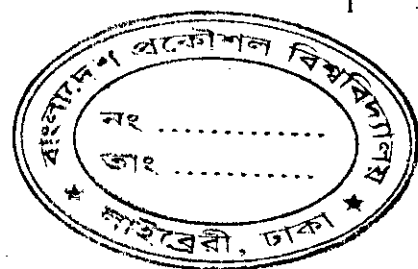
- 3.1 Schematic Diagram of the Wind Tunnel
- 3.2 Constructional Details of Cylinder
- 4.1 Section of a Cylinder Showing Pressure Tapping Position.
- 5.1 Distribution of Static Pressure Coefficient on Single Cylinder with Side Ratio ( $H/D$ ) of 0.67 at Various Nose Radius ( $r/D$ ).
- 5.2 Distribution of Static Pressure Coefficient on Single Cylinder with Side Ratio ( $H/D$ ) of 1.0 at Various Nose Radius ( $r/D$ ).
- 5.3 Distribution of Static Pressure Coefficient on Single Cylinder with Side Ratio ( $H/D$ ) of 1.5 at Various Nose Radius ( $r/D$ )
- 5.4 Typical Nature of Flow Characteristics for a sharp edged and Rounded edged Cylinders.
- 5.5 Variation of Drag Coefficient with Nose Radius ( $r/D$ ) at Side Ratio ( $H/D$ ) of 0.67 for Single Cylinder.
- 5.6 Variation of Drag Coefficient with Nose Radius ( $r/D$ ) at Side Ratio ( $H/D$ ) of 1.0 for Single Cylinder.
- 5.7 Variation of Drag Coefficient with Nose Radius ( $r/D$ ) at Side Ratio ( $H/D$ ) of 1.5 for Single Cylinder.
- 5.8 Comparison of Drag Coefficient ( $C_d$ ) for Various Side Ratios ( $H/D$ ) on Single Cylinder.
- 5.9 Static Pressure Distribution in Front Cylinder in a Group with Side Ratio ( $H/D$ ) of 0.67 and Nose Radius ( $r/D$ ) of 0.167 for various interspace ( $s/D$ ).
- 5.10 Static Pressure Distribution on Front Cylinder in a Group with Side Ratio ( $H/D$ ) of 1.0 and Nose Radius ( $r/D$ ) of 0.167 for various interspace ( $s/D$ ).
- 5.11 Static Pressure Distribution on Front Cylinder in a Group with Side Ratio ( $H/D$ ) of 1.5 and Nose Radius ( $r/D$ ) of 0.188 for Various Interspace ( $s/D$ ).
- 5.12 Static Pressure Distribution on Rear Cylinder in a Group with Side Ratio ( $H/D$ ) of 0.67 and Nose Radius ( $r/D$ ) of 0.167 for Various Interspace ( $s/D$ ).

- 5.13 Static Pressure Distribution on Rear Cylinder in a Group with Side Ratio ( $H/D$ ) of 1.0 and Nose Radius ( $r/D$ ) of 0.167 for Various Interspace ( $s/D$ ).
- 5.14 Static Pressure Distribution on Rear Cylinder in a Group with Side Ratio ( $H/D$ ) of 1.5 and Nose Radius ( $r/D$ ) of 0.188 for Various Interspac ( $s/D$ ).
- 5.15 Variation of Drag Coefficient ( $C_d$ ) with Interspace ( $s/D$ ) on Front Cylinder with Side Ratio ( $H/D$ ) of 0.67 at Nose Radius ( $r/D$ ) of 0.167.
- 5.16 Variation of Drag Coefficient ( $C_d$ ) with Interspace ( $s/D$ ) on Front Cylinder with Side Ratio ( $H/D$ ) of 1.0 at Nose Radius ( $r/D$ ) of 0.167.
- 5.17 Variation of Drag Coefficient ( $C_d$ ) with Interspace ( $s/D$ ) on Front Cylinder with Side Ratio ( $H/D$ ) of 1.5 at Nose Radius ( $r/D$ ) of 0.167.
- 5.18 Comparison of Drag Coefficient at Various Side Ratio ( $H/D$ ) on Front Cylinder.
- 5.19 Variation of Drag Coefficient ( $C_d$ ) with Interspace ( $s/D$ ) on Rear Cylinder with Side Ratio ( $H/D$ ) of 0.67 at Nose Radius ( $r/D$ ) of 0.167.
- 5.20 Variation of Drag Coefficient ( $C_d$ ) with Interspace ( $s/D$ ) on Rear Cylinder with Side Ratio ( $H/D$ ) of 1.0 at Nose Radius ( $r/D$ ) of 0.167.
- 5.21 Variation of Drag Coefficient ( $C_d$ ) with Interspace ( $s/D$ ) on Rear Cylinder with Side Ratio ( $H/D$ ) of 1.5 at Nose Radius ( $r/D$ ) of 0.188.
- 5.22 Comparison of Drag Coefficient ( $C_d$ ) on the Rear Cylinder with Interspace ( $s/D$ ) at various Side Ratios ( $H/D$ ).

## LIST OF SYMBOLS

A	Frontal Area of the cylinder
$C_d$	Drag Coefficient
$C_l$	Lift Coefficient
$C_p$	Mean Pressure Coefficient
D	Frontal Projected Width of the Cylinder
$F_D$	Drag Force per unit length of the Cylinder
$F_L$	Lift force per unit length of the cylinder
$\Delta d$	Strip width of the mid portion in the vertical direction
$\Delta h$	Strip width of the mid portion in the horizontal direction
$\Delta P_h$	Pressure differences in the horizontal strip
$\Delta P_v$	Pressure differences in the vertical strip
P	Local Static Pressure
$dp/dn$	Pressure Gradient
$P_0$	Free stream static pressure
$\Delta P$	Difference of ambient and local static pressure
u	Mean axial velocity
$U_0$	Free Stream Velocity
V	Mean wind speed at a height Z
$V_c$	Mean wind speed at the gradient height $Z_c$
x	Latitude
$\omega$	Angular Velocity of the Earth
$\alpha$	Angle of attack
$\gamma_w$	Specific weight of manometer water
$\rho$	Density of air
H/D	Side Ratio
r/D	Non-Dimensional nose radius
$R_e$	Reynolds Number
s/D	Non-Dimensional Interspace

## CHAPTER-1 INTRODUCTION



### *1.1 Background*

With the progressing world, engineering problems regarding wind loads around a group of skyscrapers, chimneys, towers and the flow induced vibration of tubes in heat exchangers, bridges, oil rigs or marine structures need detailed investigation of flow patterns and aerodynamics characteristics. Arising from the increasing practical importance of bluff body aerodynamics, there have been over the past few decades an enormous increase in research works concerning laboratory simulations, full-scale measurements and more recently numerical calculations and theoretical predictions for flows over bodies of wide variety of shapes. But the problem of wind load on building and structures is not a new one. Galileo and Newton considered the subject for study as far back as the 17th century. A number of failures of bridges, transmission towers, buildings and housings over the last one hundred years prompted researchers to do work in this field. Some of the pioneer researcher in the field are Smeaton (1759), Vogt (1880), Irminger (1891), Eiffel (1900) and Stanton (1907).

Irminger in 1891 published results of measurements on models, which was probably the first-ever wind tunnel test and Eiffel in the period up to 1900, following completion of the famous tower, conducted pioneer studies on the flow velocities and tower movements from a laboratory at the top of the tower.

The study of wind effect was first limited to loading on buildings and structures only, possibly because of its most dramatic effects are seen in their collapses. In mid-sixties researchers started the study of less dramatic, but equally important environmental aspects of the flow of wind around buildings. These include the effects on pedestrians, weathering, rain penetration, ventilation, heat loss, wind noise and air pollution etc. The pioneer researcher in this field is T. V. Lawson [36] of the University of Bristol. A number of works of the environmental aspects of wind are being studied at the Building Research Establishment at Garson and the University of Bristol, UK.

It is true that researchers from all over the world have contributed greatly to the knowledge of flow over bluff bodies [42] but the major part of the reported works are of fundamental nature involving the flow over single body of different profiles. Most of the researchers have conducted research works on either single cylindrical cylinder or a square section cylinder with various flow parameters. But the flow over either square or rectangular cylinders with rounded corners has not been studied extensively especially in-groups to date, although this is a problem of practical significance. Because it will contribute towards the knowledge of wind loads actions on groups of square or rectangular rounded buildings and structures with rounded corners.

## *1.2 Nature of the Wind*

The wind behavior is discussed in this section in brief. The characteristics of the wind, which are more or less related to the present study, have been taken into consideration for the discussion in a nutshell.

### *1.2.1 Wind Velocity:*

Winds are named by the direction they come from. Thus a wind from south, blowing toward the north is called a south wind. Windward refers to the direction a wind comes from, leeward to the direction it blows toward. When a wind blows more frequently from one direction than from any other it is called a prevailing wind. Wind speed increases rapidly with height above the ground level, as frictional drag declines. Wind is commonly not a steady current but is made up of a succession of gusts, slightly variable in direction, separated by lulls. Close to the earth the gustiness is developed due to irregularities in the wind are caused by the conventional currents. All forms of turbulence play a part in the process of transporting heat, moisture and dust into the air aloft.

There are various parameters, which control the flow behavior [12]. They are; (i) Vortices in front of the building, (ii) Opening through buildings, (iii) Spacing of rows, (iv) Wakes of buildings, (v) Long straight streets, (vi) Narrowing streets, (vii) Corners, (viii) Courtyards.

The mean wind speed varies with height. The variation of wind speed has been expressed by Davenport [19] as

$$V = V_c (Z/Z_c)^a \dots\dots\dots (1)$$

Where  $V$  is the mean wind speed at a height  $Z$ ,  $V_c$  is the mean wind speed at the gradient height  $Z_c$ . The value of  $V_c$  depends upon the geographical locality, but  $Z_c$  is a function of terrain. Values of  $Z_c$  and of the exponent "a" suggested by Davenport [19] are as follows:

- |   |   |                               |
|---|---|-------------------------------|
| - For open terrain with very few obstacles                    | : | $a = 0.16, Z_c = 300$ meters. |
| - For terrain uniformly covered with obstacles 10-15 m height | : | $a = 0.28, Z_c = 430$ meters. |
| - For terrain with large and irregular objects                | : | $a = 0.40, Z_c = 560$ meters. |

### 1.2.2 Generation of Wind:

The source of wind energy is the sun that emits solar radiation, which causes differential heating of the earth surface and the atmosphere. In the atmosphere there is a general convective transport of heat from lower to higher latitudes in order to make the earth's radiation imbalance [34]. It is for this reason that the atmosphere is a restless medium in which circulation of all sizes is normal.

Wind is simply air moving in a direction that is essentially parallel with the earth's surface. The atmosphere is fixed to the solid-liquid earth in gravitational equilibrium and so moves with the earth in its west to east rotational movement. Wind, therefore is air movement in addition to that associated with rotation. In large-scale circulation covering several thousands miles, horizontal motion greatly exceeds vertical motion. Thus, a wind that takes several-days to cross an ocean may move up or down only a few miles. The vertical component of movement is much greater in small-scale circulation such as thunderstorms and tornadoes. In a thunderstorm, air may ascend to the top of the atmosphere in about an hour.

Wind is complex in origin. Usually its direct cause lies in differences between atmospheric densities resulting in horizontal differences in air pressure. That is, it represents nature's attempt to rectify pressure inequalities. When these horizontal pressure differences develop, a gradient of pressures exists. But in spite of the direct part played by pressure differences, the

ultimate source of average for generating and maintaining winds against the drag is mainly from the differences in heating and cooling between high and low latitudes.

### **1.2.3 Forces Governing Winds:**

Four forces operate to determine the speed and direction of winds: (i) pressure gradients force, (ii) Coriolis force, (iii) Frictional force, (iv) Centrifugal force.

#### ***i) Pressure Gradient Force:***

This sets the air in motion and causes it to move with increasing speed along the gradient. The magnitude of the force is inversely proportional to the isobar spacing. Since the gradient slopes downward from high to low pressure, direction of airflow is from high to low pressure along the pressure gradient. But due to the rotation of the earth, the trajectory of an air particle moving from high to low pressure is very indirect, except close to the equator.

#### ***ii) Coriolis Force:***

This is the deflecting force of the earth's rotation that affects only the direction of wind. Except at the equator, winds and all other moving objects, no matter what their direction, are deflected to the right of the gradient in the Northern Hemisphere and to the left in the Southern Hemisphere. The force acts at right angles to the direction of motion. Coriolis force is stronger in higher latitudes. When pressure gradient is balanced by the coriolis force, wind blows parallel with the isobars and it is called geostrophic wind. The geostrophic wind  $V_c$  can be estimated from the expression as suggested by Davenport [19].

$$V_c = (dp/dn) / (2\rho\omega \cdot \sin x) \dots\dots\dots (2)$$

Where  $dp/dn$  is the pressure gradient,  $\omega$  is the angular velocity of the earth,  $x$  is the latitude and  $\rho$  is the air density.

Outside the atmosphere's friction layer may be extended up to 1000 meter above the earth's surface. Winds actually do blow in a direction almost parallel with the isobars with low pressure on the left and high pressure on the right in the Northern Hemisphere.



**iii) Frictional Force:**

This affects both wind speed and direction. Friction between the moving air and the earth's land-sea surface tends to slow the air's movement. Because of the frictional effects of the land-sea surface upon air flowing over it, surface air does not flow essentially parallel with the isobars as it does aloft, but instead crosses them at an oblique angle. The greater the friction, the wider is the angle the wind direction makes with the isobars. Winds over irregular land surfaces usually form angles varying from  $20^\circ$  to  $45^\circ$  with the isobars. But over oceans, the angle may be as little as  $10^\circ$ .

**iv) Centrifugal Force:**

This force comes into the picture only when air moves in a curved path. Centrifugal force is a major factor only when the wind is strong and the radius of curvature small as they are in tropical hurricanes, tornadoes and the centers of a few usually well-developed cyclonic storms. The flow of air which is necessary to balance pressure force, coriolis force and centrifugal force in absence of frictional force is called gradient wind. This happens at heights greater than 500 meters or so.

**1.2.4 Wind Loading on Structures:**

The development of modern materials and construction techniques has resulted in the emergence of a new generation of structures. Such structures exhibit an increased susceptibility to the action of wind. Accordingly, it has become necessary to develop tools enabling the designer to estimate wind effects with a higher degree of refinement than has previously required. It is the task of the engineer to ensure that the performance of structures subjected to the action of wind will be adequate during their anticipated life from the standpoint of both structural safety and serviceability. To achieve this end, the designer needs information regarding (i) the wind environment, (ii) the relation between that environment and the forces it induces on the structures, (iii) the behavior of the structure under the action of the forces.

The action of wind on building considering the load effect may be classified into two major groups; the static effect and the dynamic effect. There are many other effects like generation of noise the risk of the hazard, the penetration of rain and uncomfortable wind for the pedestrians etc. but they are not usually considered for structural design. Since all wind

loading are time-dependent because of varying speeds and direction of winds, wind loading are never steady. For this reason, static load is referred to the steady (time-variant) forces and pressures tending to give the structure a steady displacement. On the other hand, dynamic effect has the tendency to set the structure oscillating. A steady wind load on a building is very difficult to achieve. In fact always wind loads are of a fluctuating nature because of varying speeds and directions of winds. The type of wind and the stiffness and roughness of the structure determine the nature of loading on a building. When a building is very stiff the dynamic response of the structure may be neglected and only the static loads may be considered. This is because the natural frequency of an extremely stiff building is too high to be excited by wind. In the present study the effect of static loading is taken into account due to steady wind. Since natural winds are continually fluctuating it is generally assumed that these fluctuations are so irregular and random that the response of a structure will not differ from that due to a steady wind of the same average speed. Very recently the dynamic response of building has been considered for study because of the modern tendency to build more slender and lighter structures.

### *1.3 Importance of the Study:*

Housing and mankind is the basic primary need next to food and clothing, clear air and portable water being very essential for existence. In Bangladesh, strong wind is an annual natural hazard due to its geographical location. On the other hand, most of the existing houses and those which are going to be built in the next few decades are likely to be non-engineered, mostly with thatched roofs and are vulnerable to wind [57]. Strong wind is causing immense losses of rural dwellers by making their houses collapse fully or partially by lifting of roof etc [4]. Almost 70% of the population in the rural sector and 50% of the population in the urban sector are living below the poverty line with earnings too little to pay for all needs [14]. It is this group of people most impoverished that is to be provided with good housing. According to the recent ADB report [16] (Lewis and Chisholm), 1999, 82% of the dwellings are in rural areas. About 75% of the dwelling in rural areas are of kutchha construction (Mud, Bamboo, Woven Bamboo etc.) and that 23% of urban and more than 40% of rural dwellings are of a temporary nature. They can rarely survive against even a moderate intensity storm. Evidence from the field in strong wind-prone areas indicates that there is a socially perceived need of more engineering knowledge and improved construction of domestic dwelling [5].

The first International Conference [21] on wind effect was held in 1963 at Teddington UK where an International Study group was established from research workers, consultants and designers. Subsequent conferences had been held at four yearly intervals in Ottawa 1967 [24], Tokyo 1971 [59], London 1975 [10], and Colorado, USA 1979 so on. The conference proceedings contained results of extensive research works on "Wind Effect on Buildings and Structures"- which hitherto had been the internationally agreed title of the subject. The European title had been Industrial Aerodynamics and in North America, the term Wind Engineering had been used in the same context. At the fourth International Conference [1975], it was agreed to adopt the title Wind Engineering for all future activities.

The most serious direct effect the wind can have upon a man is to blow him over. That can cause injury and sometimes death. Two old ladies in the UK died in 1972 after being blown over by wind close to tall buildings. This kind of inconveniences was only realized after the construction of buildings that were allowed to be built by default. Very recently destructive wind tunnel testing have been conducted in Australia [1, 2] to comply with regulatory requirements of Australian Buildings.

Now-a-days the effect of wind regarding both wind loading and environmental problem is considered as one of the important design criterion in order to design a tall building in a free standing condition and as a part of a group of buildings. In Bangladesh urban environmental problems due to buildings is not yet recorded. However, the cities are rapidly growing with emphasis given to the construction of multistoried buildings to cope with the urban population pressure. The need to build in more windy sites or the need to locate a number of tall buildings close together will undoubtedly create problems not yet encountered by architects and town planners of Bangladesh.

The knowledge of wind loading on a single tall building or on a group of tall buildings is essential for sound planning and design. For designing groups of tall building, knowledge of the effect of wind loading on a group of tall buildings is essential because the interference of the neighboring buildings on a simple tall building makes the nature of wind loading different from that on a free standing building.

One approach to the problem of predicting the flow around buildings in close proximity is to develop an understanding of the nature of flows on relatively simple arrangement of bodies by Wind Tunnel experiments [53]. With these ends in view, the present investigation of pressure distributions about square or rectangular cylinders with rounded corners with varying side ratios was carried out. Square or rectangular cylinders with rounded corners ideally may represent the shape of some tall buildings. So, a study on groups of square or rectangular cylinders with rounded corners arranged simply in the staggered form would be helpful in the analysis of wind effects on some groups of buildings. This type of study may provide the engineers and architect sufficient information in choosing the shape of the tall buildings either in a freestanding condition or in a group.

Apart from wind loading problems, construction of high rise building can produce locally environmental problems like unpleasant wind conditions near ground level (e.g. blowing dust off the ground), too high wind load on people, too high speeds in streets and passages or stagnation of air in certain areas causing air pollution. Though the problem regarding the wind loading on buildings and structures is common to all parts of the world and it is expected that the solution will not be significantly different from country to country. Yet research work should be carried out in this field considering the climatic conditions and problems of this country, so that a clear picture about the nature of wind loading can be obtained applicable to our country. After all, engineers, architects and planners want to provide safe and comfortable conditions in open air pedestrian areas, and therefore need a knowledge of wind flow around rectangular rounded buildings and how to control it by good design.

#### ***1.4 Why model Study:***

Differences between wind tunnel and full-scale result can occur due to Reynolds number inequality, incorrect simulation of the atmospheric boundary layer and small-scale difference between wind tunnel and prototype model. In most wind tunnels tests the full scale Reynolds number rarely be achieved [44]. Boundary layer separation depends on Reynolds number. For sharp edged structures, separation point does not depend on Reynolds number. On the other hand the flow field around curved surfaces is very much Reynolds number dependent, so tests on these configurations must be treated with care. The crosswind scales in wind tunnels are often less than reality. This can cause underestimation of cross wind effects. The scale

difference between wind tunnel model and prototype is found in the high frequency fluctuation. High peaks found on the cladding in full-scale are not found in the wind tunnel. Those effects may be caused by structural details that are not simulated in the wind tunnel model.

After all, full-scale experiments are both costly and difficult to perform [62]. For the present study with staggered buildings full-scale experiments will not only be complex and costly but it would be difficult to record reliable pressure distributions simultaneously on the groups of buildings as there will be variation of speed and direction of wind with time. The flow around buildings in actual environment is very complex and formulation of a mathematical model to predict the flow is difficult. Thus model study is a must and the results obtained under simulated condition in the laboratory are found to be quite satisfactory for practical purposes.

### ***1.5 Aim of the Study:***

The aims of the study are as follows:

- (i) To measure the static pressure distribution around Single Square or Rectangular cylinder with rounded corners.
- (ii) To measure the pressure distributions for different side ratios (breadth / width) of cylinders.
- (iii) To measure the pressure distribution around staggered square or rectangular cylinders with rounded corners.
- (iv) To observe the effects of various inter spacing between the cylinder with various side ratios.
- (v) To determine the wind load from the static pressure distributions.
- (vi) To make comparisons of wind loads for various spacing and side dimensions of the square or rectangular cylinder with rounded corners with those with the sharp corners.

It is expected that the wind load on the square or rectangular cylinders with rounded corners will decrease appreciably compared to those with sharp edge. The results will enable the engineers and architects to design building more efficiently. Since the results will be expressed in the non-dimensional form; they will be applicable to the prototype building as well.

### ***1.6 Scope of the thesis:***

In this section a brief description of the various works which has been described in the various chapter has been taken into account.

**In chapter 1**, The wind observation has been described in short. The importance of the study has also been discussed in the chapter. The aim of the study has also been incorporated in brief.

The review of the various past works has been provided **in Chapter 2**. The works which are either directly related or a little line to the present study has been summarized in this chapter.

The experimental set-up and the measuring equipment have been provided **in Chapter 3**. The different forms of the cylinders are presented in this chapter, which are considered for the experiment.

**In Chapter 4**, The mathematical model in order to calculate the pressure coefficient, drag coefficient has been described in a nutshell. The procedure of finding the coefficients numerically from the experimental static pressure distribution values has been discussed.

**The Chapter 5** includes the most vital part of the thesis. In this chapter the results has been discussed in the most systematic way. The pressure distributions around the cylinders and the drag developed on the cylinders have been discussed elaborately.

**Finally in Chapter 6**, the conclusions from the results of the experimental investigation are given. Some recommendations are also provided for the future researchers.

## CHAPTER-2

### REVIEW OF LITERATURE

During the last half century much attention has been paid to the study of the wind loading. The occurrences of certain disastrous collapse of suspension bridges and damage to buildings and structures should not be encountered as minor criteria for design purposes. Till now extensive research work have been carried out on isolated bluff bodies. But interference with each other is a very recent endeavor. Very little information is available concerning the flow over staggered rectangular cylinders with rounded corners, although this is a problem of practical significance. The present work would be contributed towards the knowledge of wind actions on groups of buildings and structures. A brief description of some of the papers related to the present state of the problem is cited here.

Nakamura and Matskawa [45] experimentally investigated the vortex excitation of rectangular cylinders with a long side normal to the flow in a mode of lateral translation using free and oscillation methods.

Hayashi, M. Akirasakurai and Yujioha [23] made an experimental investigation into the wake characteristics of a group of flat plates consisting of two, three or four plates placed side by side normal to the flow direction.

Hua, C. K. [25] performed measurements of fluctuating lift and the oscillating amplitudes on a square cylinder in a wind tunnel test.

Okajima [48] conducted experiments in a wind tunnel and in a water tank on the vortex shedding frequencies of various rectangular cylinders.

Baines , W.D. [6] described in his paper the effects of velocity distribution on wind loads and flow patterns around buildings. He has measured pressure distributions on models of walls and rectangular block structures in a wind tunnel. Tall buildings with square sections have also been included in his study. The tests were conducted both in an artificially produced velocity gradient used to simulate natural conditions, and in a constant velocity field for comparison with standard procedures.

Matsumoto M. [41] has conducted an investigation on the aerodynamic forces acting on an oscillating square prism in a steady flow both experimentally and theoretically. First, a few experiments are performed in order to examine the aerodynamic forces, in the direction of the wind stream and in a plane normal to it, acting on an oscillating square prism. Karmon's theory about a thin plate is extended to the case of a square prism and the aerodynamic forces in a plane of the direction of the wind stream are obtained which have correlate with the experimental results fairly well.

Parkinson G.V. and Modi V.J. [49] describe in their paper about the characteristics of the separated flow over bluff two-dimensional bodies that relate to two forms of the aeroelastic instability of the bodies, vortex-excited and galloping transverse oscillation. Bodies investigated included cylinders of square, rectangular, circular, elliptical and D-section an idealized structural angle section.

Hussain H.S. and Islam O. [26] measured co-efficient of pressure and co-efficient of lift on circular, parabolic and elliptic shell roof in a uniform velocity. The investigation was performed in a small wind tunnel with Reynolds number varying between 1.7 to 350000 based on model width. The scale of the model was quite high (1:40). The variation of the Reynolds number was obtained by varying the velocity only. As the experiment was carried out in a uniform velocity, the estimated results were higher than it would be in reality.

Keffer [32] investigated the wake produced by the two-dimensional cylinder of diameters 12.7 mm, 7.93 mm and 4.76 mm with straining the flow. The tunnel speed was held constant at 5.48 m/sec so that the corresponding Reynolds number based on cylinder diameters were 4630, 2890 and 1740 for cylinder diameters of 12.7 mm, 7.93 mm and 4.76 mm respectively. The mean quantities were measured with a pitot-static tube. Experimentally he found that the wake width increased with distance along the downstream. The mean velocity distribution of the wake profile was in no way self-preserving.

Gartshore [22] investigated the two-dimensional wake of a square (6.35 mm) rod at adverse pressure gradients and at the pressure gradient for exact self-preservation. The velocity ratio was maintained approximately constant and the flow through wake having Reynolds numbers 6300 and 7300 were based on the conditions at the trailing edge.



Pearlstein A.J. Mantle W.J. [50] investigated that at low Reynolds numbers ( $Re$ ), the flow past axisymmetric and attached. For bluff bodies (e.g. spheres, mindrops and torpedoes) the flow separates as  $Re$  increases ultimately transition to unsteady axisymmetric flow becomes unstable with respect to an oscillatory helical instability at  $Re = 175.1$ . The critical  $Re$  and predicted Strouhal number (dimensionless frequency) agree well with previous experiments. We are extending this work to the case where the body falls or rises freely under the action of gravity. In that case, the rigid body motion can couple to the flow disturbances, leading to a lower critical  $Re$ .

Pearlstein A.J. Petteni F. Wang L. [51] conducted computational investigations of the stability of the steady (asymmetric) 2-D flow past a rotating cylinder, as well as the time periodic 2-D flow to which it loses its stability as the Reynolds number ( $Re$ ) is increased. To date, they have shown that the critical  $Re$  at which the steady flow becomes unstable to 2-D disturbances depends nonmonotonically on the dimensionless rotation rate, and that the frequency of the critical mode that evolves from the Hopf bifurcation has several discontinuities along the stability boundary, corresponding to transitions from one mode to another.

Pris R. [52] in his paper describes many items, one of that is the investigation of galloping oscillation on square cylinders.

Bearman P.W., and Trueman D.M. [8] investigated the base pressure co-efficient, drag co-efficient and Strouhal number of rectangular cylinders with one face normal to the flow direction. They found that when  $D/H = 0.62$ , when  $D$  is section depth and  $H$  is section width normal to the wind direction, the drag co-efficient was maximum (about 2.94). By introducing a splitter plate into the wake region they found that the increased drag effect was completely eliminated. This finding demonstrated that the high drag was associated with the regular shedding of vortices. They also showed that the further the vortices could be persuaded to form away from the body, the higher the base pressure. They suggested that for higher values of  $D/H$  ( $>0.6$ ) the vortices were forced to form further downstream because of the influence of the trailing edge corners.

Yasuhara Nakamura and Yujiohya [47] attempted to study vortex shedding from square prisms placed to smooth and turbulent approaching flows. They make flow visualization and

measured the velocity and pressure for the flow past prisms of variable length with square section. They found that square prisms shed vortices in one of the two-fixed wake planes, which were parallel with the plate sides. The plane of shedding was switched irregularly from one to the other. They further showed that the vortex shedding from a square prism with  $D/H = 0.5$  and a cube was similar, while for a square prism with  $D/H = 2.0$ , no such vortex shedding was observed.

Davis R.W. and Moore E.F. [20] carried out a numerical study of vortex, shedding from rectangular cylinders. They attempted to present numerical solutions for two-dimensional time dependent flow about rectangles in infinite domains. They investigated the initiation and subsequent development of the vortex shedding phenomena for Reynolds number varying from 100 to 2800. They found that the properties of these vortices were strongly dependent on the Reynolds number. Lift, drag and Strouhal number were also found to be influenced by Reynolds number. The computer simulation described in the paper was carried out on a UNIVAC 1108.

Lee B.E. [37] made an elaborate study of the effect of turbulence on the surface pressure field of a square prism. He presented measurements of the mean and fluctuating pressures on a square cylinder placed in a two-dimensional uniform and turbulent flow. It was observed that the addition of turbulence to the flow raised the base pressure and reduced the drag of the cylinder. He suggested that this phenomena was attributable to the manner in which the increased turbulence intensity thickened the shear layers, which caused them to be deflected by the downstream corners of the body and resulted in the downstream movement of the vortex formation region. The strength of the vortex shedding was shown to be reduced as the intensity of the incident turbulence was increased. Measurement of drag at various angle of attacks ( $0^\circ$  to  $45^\circ$ ) showed that with increase in turbulence level the minimum drag occurred at smaller values of angle of attack.

Roberson J.A., Crowe C.L. and Tseng R. [55] measured pressure distribution on rectangular rods placed in a cross flow with the rods oriented at small angle of attack with respect to the direction. The Reynolds number based on the minimum dimension of the rod was 40000 and the turbulence intensity of the cross flow ranged between 1% and 10%. They concluded that the free stream turbulence had a significant effect on the pressure distribution about bodies of rectangular cross-section. With small angle of attack these bodies had a significantly lower

pressure on their windward side wall than did the same bodies with zero angle of attack. To study the pressure distribution on bodies that more nearly represent building configurations, tests were made on bodies of square cross section placed on the floor of the wind tunnel. It was found that decreasing relative height of the body had an attenuating effect on the negative pressure on the windward side wall and it also increased the critical angle of attack.

Roberson J.A. Chi Yu Lin, Rutherford G.S. and Stine M.D. [54] carried out experiments on circular cylinders, spool shaped bodies, cup-shaped bodies, square rods and rectangular rods to observe the effect of turbulence on the drag of these bodies. For square rods with their axes parallel to the flow direction it was found the  $C_d$  decreased approximately 25% when the turbulence intensity increased from 1% to 10%. Two rectangular rods used; one had a square cross section and the other had a length (in the free stream direction) to breadth ratio of two. The drag was measured with the axes of the rectangular rods oriented normal to the free stream direction. It was noted that on the sides of the square rod the pressure change with a change in turbulence intensity was about the same as for the face: while for the rectangular rod, the change in pressure on the sides was large, and it was small on the rear face. They concluded that bodies, which have shapes such that reattachment of the flow is not a factor, experience an increase in  $C_d$  with the increased turbulence intensity. On the other hand bodies for which reattachment or near reattachment of flow occurs with increased turbulence may experience either a decrease or increase in  $C_d$  with increased turbulence intensity depending upon the shape of the body.

Barriga. A.R. Crowe C.T. and Roberson J.A. [7] studied the effects of angle of attack, turbulence intensity and scale on the pressure distribution of a single square cylinder placed in a turbulent cross flow. They found that when the square cylinder was positioned in a cross flow with one face normal to the flow direction, only drag force was produced, but in the same flow a negative lift force was developed at small positive angle of attack, the magnitude of which dependent on the turbulence characteristics of the cross flow. It was suggested that the negative lateral force on the square cylinder oriented at a small positive angle of attack was due to the relatively large negative pressure coefficient in the separated zone on the windward side wall. It was also concluded that the effect of turbulence intensity was to decrease the pressure near the front corner of the windward side wall and promote flow reattachment near the rear, giving rise to a very significant increase in aerodynamic moment.

Nakamura, Y., and Ohya, Y. [46] studied the effects of turbulence on the mean flow past square rods. Measurements were made on square rods with different lengths with their square face normal to the flow to investigate the effects of turbulence intensity and scale on the mean flow characteristics. The turbulence intensity varied from 3.5% to 13% and the length to size ratio of  $d/h$  of the rods ranged from 0.1 to 2.0 where  $d$  was the length of the rod. It was found out that there were two main effects of turbulence on the mean flow past a three-dimensional sharp edged bluff body. Small-scale turbulence increased the growth rate of the shear layer, while large-scale turbulence enhanced the roll up of the shear layer. The consequences of these demand on the shape of the bluff body. For a square plate, both small and large-scale turbulence reduced the size of the base cavity. As the length of the square rod was increased beyond the critical (0.6 times the heights), the shear layer edge direct interaction controlled the near wake eventually leading to flow reattachment. The effect of small scale turbulence was to promote the shear layer direct interaction.

Vickery B.J. [61] presented in his paper the results of the measurements of fluctuating lift and drag on a long square cylinder. He attempted to establish a correlation of lift along the cylinder and the distribution of fluctuating pressure on a cross section. It was found that the magnitude of the fluctuating lift was considerably greater than that for a circular cross section and the span wise correlation much stronger. It was also reported that the presence of large-scale turbulence in the stream had a remarkable influence on both the steady and the fluctuating forces. At small angle of attack (less than  $10^\circ$ ) turbulence caused a reduction in base suction and a decrease in fluctuating lift of about 50%.

Bostock B.R. and Mair W.A. [11] studied the pressure distributions and forces on rectangular and D-shaped cylinders placed in two-dimensional flow with a Reynolds number of 190000. It was found that for rectangular cylinders a maximum drag co-efficient was obtained when the height  $H$  (normal to the stream) of the section was about 1.5 times the width  $D$ . Reattachments on the sides of the cylinders occurred only for  $H/D$  less than 0.35.

Sakamoto H. and Arie, M. [58] collected experimental data on the vortex shedding frequency behind a vertical rectangular prism and a vertical circular cylinder attached to a plane wall and immersed in a turbulent boundary layer. They tried to investigate the effects of the aspect ratio (height / width) of these bodies and the boundary layer characteristics on the vortex

shedding frequency. Measurements revealed that two types of vortex were formed behind the body, depending on the aspect ratio, they were the arch-type vortex and the Karman-type vortex. The arch-type vortex appeared at an aspect ratio less than 2.0 and 2.5 for rectangular and circular cylinders respectively. The Karman-type vortex appeared for the aspect ratio greater than the above values. The whole experiment was conducted at a turbulence level of 0.2% and free stream velocity of 20 m/sec. The aspect ratio was varied between 0.5 to 8.0.

Castro I.P. and Robins A.G. [13] describe in their paper the flow around surface mounted cubes in both uniform, irrotational and sheared, turbulent flows. The shear flow was a simulated atmospheric boundary layers with a height ten times the body dimension. The presented measurements of body surface pressures and mean and fluctuating velocities within the wake region. These measurements reflected the effects of upstream turbulence and shear on the wake flow. It was found that in the reversed flow region directly behind the body the addition of upstream turbulence and shear considerably reduced the size of the cavity zone. Unlike the case of uniform flow the separating shear layers reattached to the body surface. Measurements for a variety of cube size boundary layer height ratios further revealed that reattachment occurred even for cube heights larger than the boundary layer height. They found that in the case of uniform flow approaching the cube at 45 degrees, the near wake and pressure fields were dominated by strong vortex shed from the top edges of the body.

Mandal A.C. [39] performed the study effect on the staggered square cylinder. The test was conducted in an open circuit wind tunnel at a Reynolds number of 27800 based on the side dimension of the square model. The maximum blockage area was 6.96 percent. Three cylinders were arranged in the staggered form (one in upstream and two in downstream flow) varying the longitudinal and transverse spacings and measurements of pressure coefficients were taken for the upstream and downstream cylinders. Experiments were also carried out for drag coefficients, lift coefficients, total force coefficients and moment coefficients. After all, it is concluded from the results that wind loading on a building is generally less severe when the building forms part of a group than when it is free-standing.

Laneville A. Gartshore I.S. and Parkinson G.V. [35] explained in their paper some effects of turbulence on bluff bodies. The bluff bodies included square and rectangular prisms.

Leutheusser J. [38] made wind tunnel tests on scale models of typical building configurations. The experiment was conducted on four models each with different height and cross section. He found out the static wind loading on each of the buildings in freestanding condition and as a member of a group of building. He concluded that the wind loading of a building was less severe when it formed a part of a group than when it was free standing.

Koeing, K. and Roshiko A. [33] described in their paper an experimental investigation of the shielding effects of various disks placed co-axially upstream of an axisymmetric flat faced cylinder. For certain combinations of the diameter and gap ratios they observed a considerable decrease in the drag of such a system. By flow visualization technique they showed that for such optimum shielding the upstream surface which separated from the disk reattached smoothly onto the front edge on the downstream cylinder.

Islam, T. [28] conducted experiments on the wind effect on the rectangular cylinders. The rectangular cylinders had side ratios of  $H/D = 1.25, 1.5, 1.75$  and  $2.0$  where  $D$  is section width normal to flow direction and  $H$  is section depth along the flow direction. The flow had a turbulence intensity of  $0.33\%$  and a constant free stream velocity of  $18.3$  m/sec was used for the purpose. It was measured mean pressure distributions around each of the cylinders for different angles of attack. He found that the form drag on the rectangular cylinder with its axis normal to the approaching flow increased with rise of the value of side ratio up to about  $0.6$ , then decreased with the further increase in the side ratio. It was also observed that the drag on an isolated cylinder was higher in general than that on the same cylinder while it becomes part of a group. The rectangular cylinder with the highest side ratio experienced minimum drag for all conditions of spacings.

Bearman P.W. and Wadcock A.J. [8] presented in their paper how the flows around two circular cylinders, displaced in a plane normal to the free stream, interact as the two bodies are brought close together. Surface pressure measurements at a Reynolds number of  $25000$  based on the diameter ( $D$ ) of a single cylinder, showed the presence of a mean repulsive force between the cylinders. At gaps between  $0.1D$  and  $1D$  a marked asymmetry in the flow was observed with the two cylinders experiencing different drags and base pressures. The base pressure was found to change from one steady value to another or simply fluctuate between the two extremes. They also showed how mutual interference influenced the formation of vortex streets from the two cylinders.

Besides these model scale and full-scale measurements on the wind loads on buildings have been performed by different authors as mentioned in the references [15], [17], [18] and [60].

## CHAPTER-3

### EXPERIMENTAL SET-UP

The investigation of wind load on the square and rectangular cylinders with rounded corners has been performed with the help of a subsonic open circuit Wind Tunnel. Four sets of square and rectangular cylinders with rounded corners have been taken into consideration in the investigation. An inclined multi-manometer was used to measure the static pressure distribution around the cylinders placed normal to the approaching uniform flow. This chapter also provides with a brief idea about the wind tunnel and its proper utilization.

#### *3.1 Measurement of Wind Characteristics:*

In the early days of aeronautics the characteristics of aerofoils, the drag of bodies and later the stability of aircraft configurations were required. The simplifications introduced by measuring forces, moments and stability on a stationary body past which wind was blown, rather than by trying to measure these quantities as the body moved through still air were released. Stanton at the National Physical Laboratory in the UK built one of the first wind tunnels in 1903 and the Wright Brothers used wind tunnel results consistently.

Over the years wind tunnel design was improved and wind tunnels become more sophisticated. Their use was applied almost exclusively to aeronautical problems and the air streams became smoother with smaller velocity profiles or distortions and the levels of turbulence were reduced to conform with the smooth flow [27].

When wind loads were first considered, a few investigations were conducted in aeronautical wind tunnels and the results were found to bear little relation to the scanty full-scale measurements available and the use of wind tunnels were filled with work on aircraft and little effort was available for a study to try to understand the causes of the differences [3]. One exception was a study by Franks in Denmark. The volume of aeronautical work in low-speed wind tunnels decreased at the end of the 1950s and in the 1960s several wind tunnel technologists turned their full-time attention to the earlier discrepancies. Davenport set up the boundary layer wind tunnel at the University of Western Ontario, Canada. Baines [6] presented a notable paper in which he explained the part played by the shear in the wind on



the flow over the front face of a bluff body, while Davenport discussed the importance of turbulence.

After all, wind is a random natural phenomenon. It can only be understood by detailed laborious measurements. Many measurement techniques in wind engineering are available. The meteorologists have been measuring the wind velocity and direction for many years. In buildings aerodynamics there are measurement techniques for pressure on buildings, and also on a small scale in wind tunnels. The instrumentation on these techniques is steel being improved with the developments of electronics. On the other hand, many comparisons in the study of the wind environment have been made and the criteria established in their forms mirror the full-scale measurements made. Melbourne [59] compares the criteria of different workers and mentions the various technologies used. Several straight comparisons between wind tunnel and full-scale measurements have been made, for example the measurements made in the Commerce Court Plaza [29]. The measurements can be divided into full scale and wind tunnel scale. A survey of possible measuring equipment is shown in Table-1.

**Table-1: A List of Different Measuring Equipment.**

Parameter	Full Scale	Wind Tunnel Scale
Wind Velocity	Cup or propeller type, anemometer, Pitot tube	Pitot tube, Hot wire Anemometer.
Wind Direction	Vane	Vane, Wool thread
Static Pressure	Static holes, Barometer	Static holes
Pressure on structure	Pressure transducers, membranes, Strain gauge based equipment.	Membranes, Water tubes, Capacitor microphones
Force	Pressure Vessel, Strain Gauge, Inductive strain measurement equipment.	Strain gauge, Aerodynamic balance.
Movements	Deflection measuring equipment, Accelerometers.	Accelerometers.

Most of the apparatus mentioned above transform the required quantity into an electric current that can be recorded and transformed into the desired data. The electrical information can be collected by a digital computer system and transformed into the required statistical

data. However, in the present investigation, wind velocity was measured with help of a digital Anemometer and by the help of an inclined manometer using water in the manometric liquid measured the static pressure distribution.

### 3.2 *Types of Wind tunnel:*

Knowledge of the types of wind tunnel might be helpful when talking to wind tunnel aerodynamicists [40]. All wind tunnels used in the study of industrial aerodynamics are "low-speed wind tunnel" whose top wind speed will probably be less than 30 m/s although most investigations will be carried out at much lower wind speeds.

Two types of wind tunnel (i) **Straight through or open return** type is a simpler form of wind tunnel which has an inlet, contraction, working section, fan, diffuser and outlet. Open return types are usually better control but higher running costs. It has a definite advantage when studying dynamic models, (ii) **Closed return type or return type** wind tunnel has continuous return. This type of wind tunnels have solid walls for their working sections. The side walls of the working section have boundary layers [32] which exercise a small effect on the flow in the main part of the working section and allowance for this presence is made by the use of blockage corrections.

### 3.3 *Specification of the Wind Tunnel:*

The schematic diagram of the experimental set-up of the present investigation has been shown in Figure 3.1. The cylinders were positioned at the exit end of the wind tunnel in the downstream. Open circuit subsonic type wind tunnel is used to develop the required flow. The tunnel is 5.93 meter long with a test section of 460 mm x 460 mm cross-section. In order to smoothen the flow a honeycomb is fixed near the end of the wind tunnel. There is a converging bell mouth shaped entry. To generate the wind velocity, two axial flow fans are used. Each of the fans is connected with the motor of 2.25 kilowatt and 2900 rpm. There is a butterfly valve to control the wind speed. There is a silencer just after the butterfly valve as shown in the figure.

The central longitudinal axis of the wind tunnel is maintained at a constant height of 990 mm from the floor. The axis of the model coincides with that of the wind tunnel. The converging

mouth entry is incorporated in the wind tunnel for smooth entry of air into the tunnel and to maintain uniform flow into the duct free from outside disturbances. The induced flow through the wind tunnel is produced by a two-stage rotating axial flow fan of capacity  $18.16 \text{ m}^3/\text{s}$  at the head of 152.4 mm of water and 1475 rpm.

A butterfly valve, actuated by a screw thread mechanism, is placed behind the fan and used to control the flow. A silencer is fitted at the end of the flow controlling section in order to reduce the noise of the system. This section is incorporated with a honeycomb. The diverging and converging section of the wind tunnel is 1550 mm long and made of 16 SWG black sheets. The angle of divergence and convergence is  $7^\circ$ , which has been done with a view to minimizing expansion and contraction loss and reducing the possibility of flow separation.

In each case of the tests, wind velocity is measured directly with the help of a digital anemometer. The flow velocity in the test section was maintained at  $14.2 \text{ m/s}$  approximately. The measured velocity distribution was uniform almost throughout in the upstream side of the models in the tunnel test section.

#### **3.4 Test Section:**

The test was done at the exit end of the wind tunnel (Figure 3.1) in the open air. In order to fix the cylinder a steel frame was manufactured, the top floor of which was at the same level of the wind tunnel at the exit end. Two side walls were attached to the steel frame at the two sides by the help of nut and bolt, so that the distance between them was equal to the distance of the side walls of the wind tunnel exit end. This distance was 450 mm. The top of the test section was kept open and at the bottom no cover plate was used. The cylinders were attached to the side walls. The side walls were made of plywood. In one side wall the cylinder was fastened by the help of nut and bolt. The bolt was fixed with one end of the cylinder. Through the other end of the cylinder, the plastic tubes were taken out in order to connect them with the inclined manometer. This end was supported in the groove of the side wall of the test section, compatible with the square or rectangular end of the cylinder. The cylinder was so positioned and fastened so that the flow direction was parallel to its sides and the front face was perpendicular to the flow direction.

To test in a group, for fixing the two cylinders one at the front and the other at the rear along the free stream direction, compatible grooves were made on the side walls of the test section. The interspace between the two cylinders was varied at 1D, 2D, 4D, 6D and 8D. With a view to achieving this, several groups were made on the side walls of the test section. When the test was conducted the unnecessary grooves were closed. The cylinders were fixed at one end by the help of bolt and nut and the other end were fixed in groove, which in attached with the square or rectangular shape of the cylinder. Through the groove as in the single cylinder the plastic tubes were taken out. They were connected to the inclined manometer. During fixing the cylinders, it was carefully checked whether the sides of the cylinders were parallel to the free stream velocity direction and the rear cylinder was just behind the front cylinder. Leveling of the testing cylinder was always checked and balanced by a standard spirit level.

### 3.5 *Constructional Details of Cylinder*

For the experimental investigation twelve square or rectangular cylinders were constructed. Of the six (three pairs) were made of side dimensions 30 mm x 30 mm ( $D=30$  mm,  $H=30$ mm). The rest six cylinders (three pairs) were made of side dimensions 45 mm x 30mm ( $D=45$  mm and  $H=30$ mm). In figure 3.2, the constructional details of the cylinders are shown. The corner of each cylinder was made rounded. The corner radii of the three pairs ( $D=30$  mm,  $H=30$  mm) were different and for each pair it was same.

For the cylinders with side dimensions  $D=30$ mm and  $H=30$ mm and side ratio ( $H/D$ ) of 1.00, the corner radii ( $r/D$ ) were 0.125, 0.167 and 0.25 based on the side  $D=30$ mm,  $D$  being the dimension perpendicular to the flow direction. Similarly for the rest three pairs of cylinders ( $D=45$  mm and  $H=30$  mm) and side ratio of 0.67, the corner radii ( $r/D$ ) were 0.125, 0.167 and 0.25 based on the side,  $D=45$  mm. These three pairs were used for the side dimensions ( $D=30$  mm and  $H=45$ mm) with side ratio ( $H/D$ ) of 1.5. As a result the corner radii were changed to 0.188, 0.25 and 0.375 based on the side  $D=30$  mm.

The cylinders were made of seasoned teakwood in order to avoid buckling, expansion and contraction due to change of temperature and humidity. As can be seen from Figure 3.2(a) one third of the cylinder length is kept solid while the rest two-third is made hollow. A bolt is welded to a steel plate, which is attached with the solid end by the help of screw. Through the hollow and plastic tubes connected to the pressure tapings are allowed to pass. They are

finally connected to the inclined manometer. Due to the limitation of the space, pressure tappings are made on the two adjacent sides only as shown in Figure 3.2(b). Four pressure tappings are made at the middle and another two tappings are made at the corners at equal interspace. The middle four tappings are placed in the same section of the cylinder while the corner tappings are placed at the different section due to space limitation. Since the flow is two-dimensional one, it is assumed that it would not make any effect in the result.

The tappings were made of copper tubes of 1.71 mm outside diameter. Each tapping was of 9 mm length approximately. From the end of the copper tube flexible plastic tube of 1.70 mm inner diameter was press fitted. Water was used as the manometric liquid.

### *3.6 Test of the Single Cylinder:*

In the first phase of the experimental investigation, the single cylinder was taken into consideration. The cylinder with side ratio ( $H/D$ ) of 0.67, 1.0 and 1.5 were used in this phase. Again for each side ratio ( $H/D$ ) three corner radius was considered. The corner radii ( $r/D$ ) were 0.125, 0.167, and 0.25 for the side ratio ( $H/D$ ) of 0.67 and 1.0 and 0.188, 0.250 and 0.375 for the side ratio ( $H/D$ ) of 1.5. First, the cylinder with side ratio ( $H/D$ ) of 0.67 ( $D=45\text{mm}$ ,  $H=30\text{mm}$ ) was placed centrally at the downstream side of the exit end of the wind tunnel. The corner radius ( $r/D$ ) was taken as 0.125. The velocity at the upstream side of the cylinder was maintained at 14.2 m/s. The velocity was measured by the help of a digital anemometer. The Reynolds number based on the frontal side dimension ( $D=45\text{mm}$ ) of the cylinder was  $4.3 \times 10^4$ . The upstream velocity was assumed to be uniform. The front side ( $D=45\text{mm}$ ) of the cylinder was oriented towards the flow direction and the top or bottom side ( $H=30\text{mm}$ ) was parallel to the flow direction. In the position the angle of attack was  $0^\circ$ . Then the static pressure distributions on the two adjacent surfaces were measured. Then the cylinder was rotated by  $180^\circ$  and the static pressure distributions on the other two faces were measured. The same test procedure was repeated to measure the static pressure distributions for the cylinders with same side ratio ( $H/D$ ) of 0.67 but corner ratios ( $r/D$ ) 0.167 and 0.250.

Next the cylinder with side ratio ( $H/D$ ) of 1.0 ( $D=30\text{mm}$ ,  $H=30\text{mm}$ ) and the corner radius ( $r/D$ ) of 0.125 was considered. The face with  $D=30\text{mm}$  was oriented towards the flow direction. The Reynolds number based on the frontal face ( $D=30\text{mm}$ ) was  $2.87 \times 10^4$  and the angle of attack was  $0^\circ$ . The measurement of static pressure distribution, was performed on the

two adjacent faces of the cylinder. Then the cylinder was rotated by  $180^\circ$  at the static pressure distributions was measured for the other two faces. In the same manner the static pressure distribution for the cylinder with side ratio of 1.0 and corner radii of 0.167 and 0.250 were taken.

Finally the cylinder with side ratio ( $H/D$ ) of 1.5 ( $D=30\text{mm}$ ,  $H=45\text{mm}$ ) was considered. The face with dimension of 30 mm was placed perpendicular to the flow direction. As a result, the Reynolds number based on the frontal face dimension of 30mm was  $2.87 \times 10^4$ . The angle of attack was  $0^\circ$ . For the three different corner radius ( $r/D$ ) of 0.188, 0.250 and 0.375 the static pressure distributions were taken in the same way as mentioned above.

### *3.7. Test of the cylinder in Group:*

In the second phase of the experimental investigation, two cylinders were used, one was at the upstream and the other was at the downstream. They were placed centrally along the flow direction. In this phase also cylinders with side ratio ( $H/D$ ) of 0.67, 1.0 and 1.5 were used. For side ratios ( $H/D$ ) of 0.67 and 1.0, the corner radius ( $r/D$ ) was considered 0.167 and for side ratio ( $H/D$ ) of 1.5, the corner radius ( $r/D$ ) was 0.188. First of all, the cylinder with side ratio ( $H/D$ ) of 0.67 was used. The angle of attack was  $0^\circ$ . The Reynolds number based on the frontal face of the cylinder ( $D=45\text{mm}$ ) was  $4.3 \times 10^4$ . The interspace between the front cylinder at the rear cylinder was taken a 1D i.e. 30mm. Then pressure distributions were measured on the four surfaces of the front and the rear cylinders. Since there were pressure tapings on the two adjacent faces of the cylinder, the cylinder was rotated by  $180^\circ$  to take the required pressure distributions on the four faces. Keeping everything identical the interspace was changed to 2D and the experiment was repeated. Next the interspace was varied to 4D, 6D and 8D and in each case the static pressure distributions on both the front and the rear cylinders were taken.

Next for the side ratio ( $H/D$ ) of 1.0 and corner radius ( $r/D$ ) of 0.167, the pressure distributions on both the front and the rear cylinders were taken in the same way as for the side ratio ( $H/D$ ) of 0.67. The interspace was varied to 1D, 2D, 4D, 6D and 8D. Then the cylinder of side ratio ( $H/D$ ) of 1.5 was considered in the experimental investigation. The pressure distributions on the front and the rear cylinders were measured for the different interspace of 1D, 2D, 4D, 6D and 8D.

## CHAPTER-4

### MATHEMATICAL MODEL

In this chapter the calculation procedure of the finding pressure coefficients and drag coefficients have been described in brief. The pressure coefficients and the drag coefficients are obtained from the numerical investigation method. Using the measured values of the pressure coefficients at the different tapping points, the expression of the pressure and the drag coefficients values are established.

#### *4.1 Calculation Procedure:*

In Figure 4.1, a cross-section of a cylinder is shown. The section has been divided both horizontally and vertically. In the vertical direction, the mid-portion has been divided into four equal strips of width  $\Delta d$  while at the corner the strip width is just half to that at the middle i.e.  $\Delta d/2$ . In the horizontal direction the width of the mid-portion is  $\Delta h$  and that at the corner is  $\Delta h/2$ . At the mid point of each middle four strips there are pressure tapings. On the other hand at the corner the tapping is not exactly at the mid-point of the strip with width  $\Delta h/2$ . It is assumed that this will make negligible error in the overall values of the pressure and drag coefficients.

Let  $\Delta P_{1h}$ ,  $\Delta P_{2h}$ ,  $\Delta P_{3h}$ ,  $\Delta P_{4h}$ ,  $\Delta P_{5h}$ , and  $\Delta P_{6h}$  are respectively the pressure differences in the horizontal direction between the opposite sides of each horizontal strip and  $\Delta P_{1v}$ ,  $\Delta P_{2v}$ ,  $\Delta P_{3v}$ ,  $\Delta P_{4v}$ ,  $\Delta P_{5v}$  and  $\Delta P_{6v}$  are the pressure differences in the vertical direction between the opposite sides of each vertical strip. Based on the length of the cylinder the area at the mid-section in the horizontal direction is  $\Delta d \times L$  and at the corner  $\Delta d/2 \times L$ . While the area in the vertical direction at the mid section is  $\Delta h \times L$  and at the corner  $\Delta h/2 \times L$ .

Now adding all the components of forces in the horizontal direction the drag forces is obtained as,

$$\begin{aligned}
F_D = & \left[ \Delta P_{1h} \times \gamma_w \times \frac{\Delta d}{2} \times L + \Delta P_{2h} \times \gamma_w \times \Delta d \times L + \Delta P_{3h} \times \gamma_w \times \Delta d \times L + \Delta P_{4h} \times \gamma_w \times \Delta d \times L \right. \\
& + \left. \Delta P_{5h} \times \gamma_w \times \Delta d \times L + \Delta P_{6h} \times \gamma_w \times \frac{\Delta d}{2} \times L \right] \times g \cos \alpha + \left[ \Delta P_{1v} \times \gamma_w \times \frac{\Delta h}{2} \times L + \Delta P_{2v} \times \gamma_w \times \Delta h \times L \right. \\
& + \left. \Delta P_{3v} \times \gamma_w \times \Delta h \times L + \Delta P_{4v} \times \gamma_w \times \Delta h \times L + \Delta P_{5v} \times \gamma_w \times \Delta h \times L + \Delta P_{6v} \times \gamma_w \times \frac{\Delta h}{2} \times L \right] g \sin \alpha \quad (1)
\end{aligned}$$

The lift force is determined from

$$\begin{aligned}
F_L = & \left[ \Delta P_{1h} \times \gamma_w \times \frac{\Delta d}{2} \times L + \Delta P_{2h} \times \gamma_w \times \Delta d \times L + \Delta P_{3h} \times \gamma_w \times \Delta d \times L + \Delta P_{4h} \times \gamma_w \times \Delta d \times L \right. \\
& + \left. \Delta P_{5h} \times \gamma_w \times \Delta d \times L + \Delta P_{6h} \times \gamma_w \times \frac{\Delta d}{2} \times L \right] \times g \sin \alpha + \left[ \Delta P_{1v} \times \gamma_w \times \frac{\Delta h}{2} \times L + \Delta P_{2v} \times \gamma_w \times \Delta h \times L \right. \\
& + \left. \Delta P_{3v} \times \gamma_w \times \Delta h \times L + \Delta P_{4v} \times \gamma_w \times \Delta h \times L + \Delta P_{5v} \times \gamma_w \times \Delta h \times L + \Delta P_{6v} \times \gamma_w \times \frac{\Delta h}{2} \times L \right] g \cos \alpha \quad (2)
\end{aligned}$$

Equation (1) may be written as,

$$\begin{aligned}
F_D = & \gamma_w \times \Delta d \times L g \left[ \frac{\Delta P_{1h}}{2} + \Delta P_{2h} + \Delta P_{3h} + \Delta P_{4h} + \Delta P_{5h} + \frac{\Delta P_{6h}}{2} \right] \cos \alpha \\
& + \gamma_w \times \Delta h \times L g \left[ \frac{\Delta P_{1v}}{2} + \Delta P_{2v} + \Delta P_{3v} + \Delta P_{4v} + \Delta P_{5v} + \frac{\Delta P_{6v}}{2} \right] \sin \alpha \quad (3)
\end{aligned}$$

Which can be expressed as,

$$F_D = \gamma_w \times L g [\Delta d \Delta p_h \cos \alpha + \Delta h \Delta p_v \sin \alpha] \quad (4)$$

$$\text{where, } \Delta p_h = \frac{\Delta P_{1h}}{2} + \Delta P_{2h} + \Delta P_{3h} + \Delta P_{4h} + \Delta P_{5h} + \frac{\Delta P_{6h}}{2} \quad (5)$$

$$\Delta p_v = \frac{\Delta P_{1v}}{2} + \Delta P_{2v} + \Delta P_{3v} + \Delta P_{4v} + \Delta P_{5v} + \frac{\Delta P_{6v}}{2} \quad (6)$$

Writing  $\Delta d = \Delta L$  and  $\Delta h = (H/D) \Delta L$  and substituting in equation (4), drag force can be expressed as,

$$F_D = \gamma_w \times \Delta L \times L g \left[ \Delta p_h \times \cos \alpha + \left( \frac{H}{D} \right) \times \Delta p_v \times \sin \alpha \right] \quad (7)$$

Which can be written as,

$$F_D = \gamma_w \times \Delta L \times L \times g [\Delta P_D] \quad (8)$$

$$\text{where, } \Delta P_D = \Delta p_h \cos \alpha + \left( \frac{H}{D} \right) \Delta p_v \sin \alpha \quad (9)$$

When the value of angle of attack becomes zero, the  $\Delta P_D$  is obtained from,

$$\Delta P_D = \Delta p_h \quad (10)$$



In the same way, the expansion of the lift force  $F_L$  is found as,

$$F_L = \gamma_w \times \Delta L \times L g [\Delta p_L] \quad (11)$$

$$\text{when, } \Delta P_L = \Delta P_h \sin \alpha + (H/D) \Delta P_v \cos \alpha \quad (12)$$

When the angle of attack becomes zero,  $\Delta P_L$  is reduced to,

$$\Delta P_L = (H/D) \times \Delta P_v \quad (13)$$

$$\text{Drag co-efficient is defined as, } C_d = \frac{F_D}{\frac{1}{2} \rho A U_o^2} \quad (14)$$

Where,  $U_o$  is the free stream velocity.

Equation (14) may be written as substituting the value of  $F_D$  from equation (8)

$$C_d = \frac{\gamma_w \times \Delta L \times L \times g \times \Delta P_D}{\frac{1}{2} \rho \times 5 \Delta L \times L \times U_o^2} \quad (15)$$

$$\text{The lift coefficient is defined as, } C_l = \frac{F_L}{\frac{1}{2} \rho A U_o^2} \quad (16)$$

Which can be written as, substituting the value of  $F_L$  from equation (11)

$$C_l = \frac{\gamma_w \times \Delta L \times L \times g \times \Delta P_L}{\frac{1}{2} \rho \times 5 \Delta L \times L \times U_o^2} \quad (17)$$

Equation (15) and (17) are reduced to the form,

$$C_d = \frac{\gamma_w \times g \times \Delta P_D}{2.5 \rho U_o^2} \quad (18)$$

$$\text{and } C_l = \frac{\gamma_w \times g \times \Delta P_L}{2.5 \rho U_o^2} \quad (19)$$

Pressure co-efficient is defined as,

$$C_p = \frac{P - P_o}{\frac{1}{2} \rho U_o^2} \quad (20)$$

Where,  $P_o$  is the ambient pressure

$P$  is the static pressure on the surface of the cylinder.

$\rho$  is the density of the air = 1.22 kg/m<sup>3</sup>.

Equation (20) may be rewritten in the form,

$$C_p = \frac{\Delta P}{\frac{1}{2} \rho U_o^2} \quad (21)$$

The value of  $\Delta P$  is obtained from,

$$\Delta P = K \Delta h \times \gamma_w \times g$$

Where,  $\Delta h$  is the manometer reading.

K is a constant.

$\gamma_w$  is the sp. weight of manometric fluid.

#### 4.2 Sample Calculation:

The Coefficient of Pressure ( $C_p$ ) can be calculated as,

$$\begin{aligned} C_p &= \frac{\Delta P}{\frac{1}{2} \rho U_o^2} & (21) \\ &= \frac{\frac{\Delta h \times 25.4}{1000} \times 1000 \times 9.81}{\frac{1}{2} \times 1.22 \times U_o^2} \\ &= \frac{25.4 \times 9.81 \times 2 \left( \frac{\Delta h}{U_o^2} \right)}{1.22} \\ &= 408.482 \left( \frac{\Delta h}{U_o^2} \right) \\ &= \frac{408.482}{(14.2)^2} \Delta h = 2.026 \Delta h \end{aligned}$$

The Coefficient of drag ( $C_d$ ) can be calculated from,

$$C_d = \frac{g \gamma_w \Delta P_h}{2.5 \rho U_o^2} \quad (18)$$

For set-1, Cylinder dimensions: 30 mm x 45 mm, Nose radius,  $r = 11.25$  mm,  $H/D=1.5$ ,  $r/D=0.375$

$$C_d = \frac{\Delta P_h \times \gamma_w \times g}{2.5 \times 1.22 \times (14.2)^2} = \frac{1.696 \times 25.4}{2.5 \times 1.22 \times (14.2)^2} \times 1000 \times 9.81 = 0.687$$

where,

$$\begin{aligned} \Delta P_h &= \frac{-0.49 + 0.26}{2} + (0.301 + 0.19) + (0.53 + 0.16) + (0.36 + 0.13) + (0.3 + 0.18) + \left( \frac{-0.48 + 0.2}{2} \right) \\ &= -0.115 + 0.491 + 0.49 + 0.49 + 0.48 - 0.14 \\ &= 1.696 \text{ inch. of } H_2O = \frac{1.696 \times 25.4}{1000} \text{ m of } H_2O. \end{aligned}$$

Since the value of angle of attack was maintained at zero, and the cylinder was so arranged that the static pressure on the top and the bottom surfaces were symmetric [56]. So the net lift

force was zero; for the present configuration of the cylinder either for the single or the group consisting of two cylinders one at the front and the other at the rear along the flow direction.

## CHAPTER-5

### RESULTS AND DISCUSSIONS

The results of the experimental investigation in regard to distributions of static pressure coefficient on the square and the rectangular cylinders with rounded corners have been discussed in this chapter. First of all the distributions of the static pressure coefficient on the single cylinder with different side ratios and nose radius are taken into consideration. Then the distributions of the static pressure coefficient on the cylinders in a group are considered. The results based on the various inter-space of the cylinders in the group are discussed elaborately. The calculated drag coefficients from the measured static pressures for both the single cylinder and the cylinders in the group are also discussed.

#### 5.1 Single Cylinder

In this section distributions of the static pressure coefficients and the drag coefficients have been taken into consideration for discussion. The static pressure coefficients are obtained from the measured static pressures. The drag coefficients, which are calculated from the pressure coefficients, are also discussed.

##### 5.1.1 Static Pressure Coefficient

In Figures 5.1 to 5.3, the distributions of the static pressure coefficients on the single cylinder have been presented. The static pressure coefficients with side ratio ( $H/D$ ) of 0.67 at the different nose radii ( $r/D$ ) have been shown in Figure 5.1. The side dimension of the cylinder perpendicular to the flow direction was 45 mm. Based on this side dimension the Reynolds number is  $4.30 \times 10^4$ . The flow was considered to be uniform in the upstream side of the cylinder. The angle of attack of the flow was  $0^\circ$ . It can be seen from this figure that the static pressure coefficients at the different nose radii change negligibly. Since the flow is symmetric over the cylinder the distribution of the pressure coefficients on the top and bottom are more or less identical. At the front side the static pressure coefficients near the middle approaches to unity due to stagnation effect. The pressure coefficients at the corner are seen to be negative. It is observed from this figure that the distribution of the pressure coefficient at the rear is of almost uniform nature. The velocity in the wake

region is much lower than the mean flow as suggested by Baines [6], as a result the nature of the pressure coefficient becomes of the uniform nature.

For the flow over the cylinder with rounded corner there is no fixed separation point as in the case of a cylinder with the sharp edge where the separation point is fixed and it occurs just at the sharp edge. For the cylinder with rounded corner the separation point proceeds towards the downstream side. One can see the typical nature of the separation for the cylinder with the sharp edge and the rounded corner from Figure 5.4. A pair of vortices is generated at the downstream side of the cylinder. One rotates in the clockwise direction and the other rotates in the anti-clockwise direction. The distance of the pair of the vortices from the rear side of the cylinder depends on the corner configuration of the cylinder, which can be observed from this figure. It can be further noticed from this figure that the lateral distance of the two vortices also depends on the corner configuration. The location of the separation point and the distance of the pair of the vortices are the controlling factor of the values of the pressures on the top, bottom and the rear faces of the cylinder. It can be noticed from Figure 5.1 that the values of the pressure coefficients at the different nose radii change negligibly which may be due to the locations of the separation points at the close proximity for the different values of the nose radii. One can observe from this figure that at the top and bottom near the mid section there appear some pressure recovery which may be due to the effect of the some reattachment in that region.

In Figure 5.2, distribution of static pressure coefficients with side ratio ( $H/D$ ) of 1.0 at various nose radii is presented. The pressure coefficients distribution for the cylinder with the sharp corner provided by Mandal and Islam [39, 28] is also given for comparison. The Reynolds number based on the front side dimension is  $2.87 \times 10^4$ . The angle of attack of the flow is  $0^\circ$ . As can be seen from the figure that for the cylinder with sharp edge corner the values of the negative pressure coefficients are much higher i.e. pressure decreases. For the cylinder with rounded corner the pressure coefficients increase. This may happen because of the fact that for the cylinder with rounded corner the separation point proceeds towards the downstream side in comparison to that for the cylinder with sharp edge, as a result the position of the pair of the vortices occurs in the downstream side compared to that for the cylinder with sharp edge. One can see this feature from figure 5.4. The longer is the distance of the pair of the vortices from the body, higher is the pressure at the rear side and vice versa.

It can be further noticed from Figure 5.2 that there is minor effect of the nose radius on the pressure coefficient values. At all the nose radii the pressure coefficient values are close and uniformly distributed at the top, bottom and rear sides indicating that the separation point at all the nose radius may remain close to each other.

The distributions of the static pressure coefficients with side ratio ( $H/D$ ) of 1.5 at various nose radii ( $r/D$ ) have been shown in Figure 5.3. In this figure the distribution of the pressure coefficients for the cylinder with sharp edge presented by Islam and Mandal [28,39] is also given for comparison. The Reynolds number based on the front side dimension of the cylinder is  $2.87 \times 10^4$ . It is seen from the figure that the negative values of the pressure coefficients for the cylinder with sharp edge are remarkably higher than those for the cylinder with rounded corner. This nature can be explained in the same way as for Figure 5.2. For the different nose radii the pressure coefficients do not vary much. At the top and bottom towards the downstream side some pressure recovery occur which may be due to some reattachment. At the backside also at the mid section some pressure recovery is observed from the nature of the pressure coefficient distribution.

### 5.1.2 Drag Coefficients

In Figures 5.5 to 5.7 the variations of drag coefficient with nose radius ( $r/D$ ) for different side ratios of 0.67, 1.0 and 1.5 respectively have been presented. It can be observed from this figure that in each case with the increase of the nose radius the drag coefficient decreases. It can be further noticed from these figures that with the increase of the nose radius the drag coefficient decrease but with further increase of the nose radius no remarkable change in the drag coefficient occurs. Since the pressure coefficients values increase at the back face of the cylinder with the nose radius the drag coefficient decreases.

Comparisons of the drag coefficients for various side ratios ( $H/D$ ) of 0.67, 1.0 and 1.5 have been shown in Figure 5.8. The calculated result of the drag coefficient from the present empirical equation of the drag coefficient for the single cylinder with different nose radius is also provided for comparison. One can see from this figure that there is

good correlation of the experimental results of the drag coefficients and the calculated values by the empirical relation.

### **Imperial Relationship of Drag Coefficient ( $C_d$ ) with Nose Radius ( $r/D$ ):**

An empirical relation of the drag coefficient for the single cylinder as a function of nose radius has been introduced as,

$$C_d = 10 (r/D)^2 - 7.25(r/D) + 2.0; \quad \text{for } r/D < 0.4 \dots\dots\dots (22)$$

There is some effect of the side ratio of the cylinder, which can be observed from Figure 5.8.

## **5.2 Cylinders in a Group**

In this section the distributions of the static pressure coefficients on the cylinder in a group are discussed. The group consists of two cylinders, one at the upstream and the other at the downstream side just behind the upstream cylinder along the flow direction. The drag coefficient on the cylinder is also discussed. The effect of the inter-space of the two cylinders on the static pressure coefficients and the drag coefficients has been discussed elaborately.

### **5.2.1 Static pressure Coefficients**

The distributions of the static pressure coefficients on the front cylinder in a group with rounded corner are shown in Figures 5.9 to 5.11. In Figure 5.9, the distributions of the static pressure coefficients on the front cylinder with side ratio ( $H/D$ ) of 0.67 and nose radius ( $r/D$ ) of 0.167 has been presented. The pressure coefficients at the different inter-space ( $s/D$ ) of 1, 2, 4, 6 and 8 between the upstream and the downstream cylinders are given in this figure. The Reynolds number based on the front side dimension of the cylinder was  $4.30 \times 10^4$  and the angle of attack was  $0^\circ$ . One can observe from the pressure coefficients distribution on the front face that at inter-space of 1.0, the values of the pressure coefficients in the middle is almost unity whereas with the further increase of the inter-space ( $s/D$ ) value, the pressure coefficients decrease.

It is seen from this figure that on the top and bottom the pressure coefficients values are almost identical due to the symmetry of the flow. In general the values of the pressure coefficients increase by some amount with the increase of the inter-space on the top, bottom and the rear faces of the cylinder. Comparing the pressure coefficients from the figures 5.1 and 5.9 it is evident that due to the presence of the cylinder at the downstream side the back pressure of the front cylinder in the group increases in respect to that for the single cylinder. The recovery of the pressure occurs due to the presence of the downstream cylinder. The flow at the downstream of the front cylinder is influenced for the presence of the downstream cylinder. The flow at the downstream of the front cylinder becomes more turbulent resulting relatively more mass and momentum transfer which creates pressure recovery on the top, bottom and the back of the upstream cylinder.

The distributions of the pressure coefficients on the front cylinder of the group with side ratio ( $H/D$ ) of 1.0 and nose radius ( $r/D$ ) of 0.167 at various inter-space ( $s/D$ ) of 1, 2, 4, 6 and 8, have been presented in Figure 5.10. It can be seen from this figure that at the different inter-space the values of the pressure coefficients are close with each other. If the pressure coefficients values are compared in Figures 5.2 and 5.10, it appears that there is small effect on the pressure coefficient distribution on the front cylinder due to the presence of the cylinder at the downstream side in the group. It is also clear from Figure 5.10 that there is very small effect of the inter-space on the results.

In Figure 5.11 the distributions of the pressure coefficients on the front cylinder with side ratio ( $H/D$ ) of 1.5 and nose radius of 0.188 at different inter-space ( $s/D$ ) of 1, 2, 4, 6 and 8, are shown. The nature of the distributions of the pressure coefficients is similar to that on the front cylinder in Figure 5.10. The effect of the inter-space is also very insignificant as can be seen from the figure.

Static pressure distributions on the rear cylinder in the group with side ratio ( $H/D$ ) of 0.67 and nose radius ( $r/D$ ) at various inter-space ( $s/D$ ) of 1, 2, 4, 6, and 8 are presented in Figure 5.12. It can be seen from this figure that on the top and bottom the pressure distributions are of identical nature due to the symmetry of the flow. In the front face at the small inter-space the pressure coefficients become negative while at the higher inter-space there appears slight positive pressure coefficient. It is seen from this figure that on



the top, bottom and the back surfaces of the cylinder there are negligible variation of pressure coefficients for the different inter-space values. It can be further observed from this figure that the values of the pressure coefficients at the top, bottom and the back sides of the cylinder are much higher than those for the single cylinder (Figure 5.1).

The front surface of the downstream cylinder remains in the wake region completely produced by the upstream cylinder. As the inter-space becomes closer relatively larger wakes are generated. The flow on this face never becomes potential as it occurs in the case of the single cylinder. The velocity with which the flow occurs on the front face of the single cylinder is much greater than the mean velocity of the flow with which it occurs on the front face of the downstream cylinder in the group. The mean velocity in the wake is much lower than the free stream velocity. For these reasons the values of the pressure coefficients become negative on the front face of the downstream cylinder at the low inter-space ( $s/D$ ) of 1 and 2. While at the higher inter-space ( $s/D$ ) of 4, 6 and 8 some positive values are found to develop.

At the top, bottom and the back faces the pressure coefficients become much higher than those for the single cylinder which may be for the higher turbulent nature of flow on these faces due to the presence of the upstream cylinder. For the higher turbulent mass and momentum transfer becomes higher resulting pressure recovery on these faces.

Static pressure distributions on the rear cylinder in a group with side ratio ( $H/D$ ) of 1.0 and nose radius ( $r/D$ ) of 0.167 for various inter-space ( $s/D$ ) of 1, 2, 4, 6 and 8 have been shown in Figure 5.13. One can see from this figure that on the front face of the cylinder the pressure coefficients become negative while at the higher inter-space positive pressure coefficients are obtained. Still the values of the pressure coefficients are much lower than unity. This face remains in the wake region for its position in the downstream side of the front cylinder in the group. The mean velocity of the wake is lower as a result the values of the pressure coefficients are lower. With the higher inter-space the influence of the upstream cylinder decreases making the higher values.

On the top and the bottom faces the nature of the distribution are identical because of the symmetric flow. It can be noticed from this figure that on the top, bottom and the back

faces the pressure coefficients do not depend much on the inter-space of the two cylinders. However, the values of the pressure coefficients are higher than those of the single cylinder. For the higher turbulent nature of flow due to the presence of the upstream cylinder there occurs pressure recovery on these faces making higher values of the pressure coefficients.

In Figure 5.14 distributions of static pressure coefficients on the rear cylinder in a group with side ratio ( $H/D$ ) of 1.5 and nose radius ( $r/D$ ) of 0.188 for various inter-space ( $s/D$ ) are presented. On the front face of the cylinder all the values of the pressure coefficients are positive. With the increase of the inter-space the pressure coefficients become relatively higher. As the inter-space increase the influence decreases, still the pressure coefficient values are much lower than unity. It can be explained in the same way as for the Figure 5.13. One can observe from this figure that the effect of the inter-space on the distributions of the pressure coefficients on the top, bottom and the back faces is negligible. On these faces the values of the pressure coefficients are much higher than those for the single cylinder. It is due to higher turbulent nature of flow on these faces making recovery of the pressure appreciably.

### 5.2.2 Drag Coefficients

Variation of drag coefficients ( $C_d$ ) with inter-space ( $s/D$ ) on the front cylinder with side ratio ( $H/D$ ) of 0.67 and at nose radius ( $r/D$ ) of 0.167 is shown in Figure 5.15. It is seen from this figure that with the increase of the inter-space the drag coefficient decreases by some amount. Since the back pressure increases on the front cylinder with the increase of the inter-space as can be seen from Figure 5.9, the drag coefficient decreases.

In Figure 5.16, the variation of drag coefficient ( $C_d$ ) with inter-space ( $s/D$ ) on the front cylinder with side ratio ( $H/D$ ) of 1.0 at nose radius ( $r/D$ ) of 0.167 is presented. It can be observed from this figure that with the increase of the inter-space the drag coefficient decreases but not appreciably. The variation of drag coefficient ( $C_d$ ) with inter-space ( $s/D$ ) on the front cylinder with side ratio ( $H/D$ ) of 1.5 at nose radius ( $r/D$ ) of 0.167 is shown in Figure 5.17. One can notice from this figure that there is some effect of the inter-space on the drag coefficient. With the increase of the inter-space the drag coefficient decreases.

Comparison of drag coefficients at various side ratios ( $H/D$ ) on the front cylinder is shown in Figure 5.18. It is evident from this figure that there is some effect of the side ratio on the drag coefficients. At the side ratio of 1.5 the drag coefficients are lower. This behavior can be explained from the pressure coefficient distributions on the relevant cylinders. It can be further noticed from Figure 5.18 that with the variation of the inter-space drag coefficient values do not change much. The values of the drag coefficients are distributed around 1.0. In comparison to the drag coefficient of the single cylinder the drag coefficient on the front cylinder in the group do not change much.

In Figure 5.19 variation of drag coefficient ( $C_d$ ) with inter-space ( $s/D$ ) on the rear cylinder in the group with side ratio ( $H/D$ ) of 0.67 and nose radius ( $r/D$ ) of 0.167 is shown. It can be seen from this figure that there is wide variation of the drag coefficient for the different inter-space ( $s/D$ ). One important point can be noticed from this figure that at the lower inter-space the drag coefficient becomes even negative. However, for the higher inter-space the drag coefficient becomes positive but not much higher as for the single cylinder. The presence of the upstream cylinder reduces the drag significantly on the rear cylinder. It can be explained from the pressure distributions on this cylinder.

Variation of the drag coefficient ( $C_d$ ) with inter-space ( $s/D$ ) on the rear cylinder with side ratio ( $H/D$ ) of 1.0 and nose radius ( $r/D$ ) of 0.167 is presented in Figure 5.20. It is seen from this figure that the effect of the inter-space on the drag coefficient is remarkable. At the lower value of the inter-space the drag coefficient becomes negative and as the inter-space increases the value of drag coefficient increases and becomes positive. But still the value remains much lower than that on the single cylinder.

In Figure 5.21 variation of drag coefficient ( $C_d$ ) with inter-space ( $s/D$ ) on the rear cylinder with side ratio ( $H/D$ ) of 1.5 and the nose radius ( $r/D$ ) of 0.188 is presented. There is significant effect of the inter-space on the drag coefficient on the rear cylinder as can be seen from Figure 5.21. Except at inter-space of 1, at all the other inter-spaces the drag coefficient is positive but much lower than that on the single cylinder.

Finally in Figure 5.22 comparison of drag coefficients on the rear with inter-space ( $s/D$ ) at various side ratios ( $H/D$ ) is shown. It is observed from this figure that there is some effect of the side ratio on the drag coefficient on the rear cylinder.

It may be mentioned here that the investigation of the drag coefficient on the cylinders in the group has been made with the single nose radius value. From the result of the drag coefficient on the single cylinder it is noticed that with the higher values of the nose radius no prominent change in the drag coefficient is found. As a result only single value of the nose radius has been taken into consideration for the study on the group of the cylinders.

## CHAPTER-6

### CONCLUSIONS AND DISCUSSIONS

#### 6.1 Conclusions:

The following conclusions are drawn in regard to the flow on the single square or rectangular cylinder and the square or rectangular cylinders in a group with rounded corners:

1. For the rounded corner of the square or rectangular cylinder the drag coefficients values decrease remarkably than those for the cylinder with sharp edge.
2. With the increase of the nose radius the drag coefficient decreases but with further increase of nose radius, no appreciable change in drag coefficient is found.
3. The effect of side ratio ( $H/D$ ) on the drag coefficient is not significant.
4. There is small effect of the inter-space ( $s/D$ ) between the upstream and the downstream cylinders on the drag coefficient of the upstream cylinder in the group.
5. Significant effect of the inter-space ( $s/D$ ) is observed on the drag coefficient of the downstream cylinder in the group.
6. It appears from the investigation that there would be lower wind load on a building, which will remain in the wake region produced by the building in the group.
7. Since from the investigation it is evident that after certain nose radius no further remarkable decrease in the drag coefficient is found, it may be taken into consideration by the relevant architect and engineers during performing their designs.
8. The outcome of the results may be applied for the design of the group of buildings while considering wind load [31].
9. The stagnation point is found on the front face of either the single cylinder or the upstream cylinder in a group but on the front face of the downstream cylinder in a group no such stagnation point is found.

## 6.2 Recommendations:

For the further study in relation to the present work the following recommendations are provided below:

1. The experimental investigation may be conducted with the cylinder of elliptical cross-section.
2. The flow is considered to be uniform in the present study. The investigation may be repeated considering the different values of the turbulence intensity specially the atmospheric turbulence level..
3. The flow behavior around the cylinder may be taken into consideration for the study.
4. The wind shear may be considered in performing the study to see its effect on the wind load.
5. The effect of the Reynolds number may be investigated on the wind load of the single as well as cylinders in a group.
6. The study in regard to the optimum inter-spacing between the tall buildings, which is suitable to the passers-by, may be performed.
7. Building models with different spacing of various shapes and sizes may be considered to find the wind load on them.

## REFERENCES

- [1] **Ahmed, N.A. and Back, J.**(1996) Destructive Wind Tunnel Tests, UNSW Unisearch Report no.23214-10, Australia, 1996.
- [2] **Ahmed, N.A. and Back, J.**(1997) Wind Tunnel Tests on Two Vevtilators, UNSW Unisearch Report no.29295-01, Australia, 1997.
- [3] **Allen, H.J. and Vincent, W.G.** "Wall interference in a Two-dimensional Flow Wind Tunnel", NACA Report No. 782.
- [4] **Anthony, K.C.** "Wind Engineering- The personal view of a practicing Engineer", "Proceedings of the Fourth International Conference on Wind Effects on Buildings and Structures", London, U.K. 1975, P.765-772.
- [5] **Anwar, AMMT** (1996), Wind Resistance on Non Engineered Housing. In Implementing Hazard-Resistance Housing, Proceeding of the Ist International Housing and Hazards Workshop to Explore Practical Building for Safety Solutions held in Dhaka, Bangladesh, 3-5 December 1996, Edited by Hodgson, Seraj and Chowdhury, pp.11-17.
- [6] **Baines, W.D.**, "Effects of Velocity Distribution on Wind Loads and Flow Patterns on Buildings", Proceedings of a Symposium on Wind Effects on Buildings and Structures," Teddington, U.K, 1963, pp.197-225.
- [7] **Barriga, A.R., Crowe, C.T. and Roberson, J.A.**, "Pressure Distributions on a Square Cylinder at a Small Angle of Attack in a Turbulent Cross Flow", Proceedings of the 4th International conference on Wind Effects on Buildings, London, U.K. 1975,pp.89-93.
- [8] **Bearman P.W. and Truman, D.M.**, "An Investigation of the Flow Around Rectangular Cylinders", The Aeronautical Quarterly, Vol.23, 1971, p.229-237.
- [9] **Bearman, P.W. and Wadcock, A.J.**, "The Interaction Between a Pair of Circular Cylinders Normal to a Stream", Journal of the Fluid Mechanics, Vol. 61, 1973, p.499-511.
- [10] **Bostock, B.R. and Mair, W.A.**, "Pressure Distributions and Forces on Rectangular and D-shaped Cylinders", The Aerodynamical Quarterly , Vol.23, 1972, pp.499-511.
- [11] **Bradbury, L.J.S.**, "Pulsed wire anemometer measurements on the flow past a normal flat plate in uniform and sheared flow", 4th Int. Conf. on Wind Effects on Buildings and structures," Heathrow 1975, Cambridge University Press.
- [12] **Castro, I.P. and Fackrell, J.E.**, " A Note on Two-Dimensional Fence Flows with Emphasis on Wall Constraint", J. Indust. Aerodynamics, 3(1), March 1978.

- [13] **Castro, I.P. and Robins, A.G.**, "The Flow Around a Surface Mounted Cube in Uniform and Turbulent Streams", *Journal of Fluid Mechanics*, Vol.79, 1977, pp.305-335.
- [14] **Chowdhury J.R.**, (1996), BNBC (1993), Bangladesh National Building Code, 1993 HBRI-BSTI, Design and construction of Houses to Resist Natural Hazards. In *Implementing Hazard Resistance Housing*, Proceedings of the 1st International Housing and Hazards Workshop to Explore Practical Building for Safety Solutions held in Dhaka, Bangladesh, 3-5 December 1996, Edited by Hodgson, Seraj and Chowdhury, pp.11-17.
- [15] **Cheung, J.C.K., Holmes, J.D., Melbourne, W.H., Lakshmanan, N. and P. Bowdith**, "Pressures on a 1:10 Scale Model of the Texas Tech Building", *J. Wind Eng. Ind. Aerodyn.* no.69-71, 1997, pp.529-538- Proceedings of the Journal of the Institutions of Engineers (India), Volume-83, June 2002.
- [16] **Chisholm, M.P. and Lewis, J.**, (1996) Cyclone-Resistance domestic Construction in Bangladesh. In *Implementing Hazard Resistance Housing*, Proceeding of the 1st International Housing and Hazards Workshop to Explore Practical Building for Safety Solutions held in Dhaka, Bangladesh, 3-5 December 1996, Edited by Hodgson, Seraj and Chowdhury, pp.29-38, NBS (1977), 43 Rules. How Houses can better Resist High Wind, US National Bureau of Standards, Washington DC.
- [17] **Cochran L.S. and Cermak J.E.**, "Full and Model Scale Cladding Pressures on the Texas Tech University Experimental Building," *J. Wind Eng. Ind. Aerodyn.* no.43, 1992, pp.1589-1600.
- [18] **Coudrey, C.F.**, "The application of Maskell's Theory of Wind Tunnel Blockage in every large Solid Models", NPL-Aero Report 1247, HMSO, October 1957.
- [19] **Davenport, A.G.**, "The Relationship to Wind Structure to Wind Loading", "Proceedings of the Conference on Wind Effects on Buildings and Structures", Vol. 1, June, 1963.
- [20] **Davis, R.W and Moore, E.F.**, "A Numerical Study of Vortex Shedding from Rectangular Cylinder," *Journal of Fluid Mechanics*, Vol. 116, p. 475-506.
- [21] **Franck, N.**, Model Law and Experimental technique for determination of Wind Loads on Buildings," 1st Int. Conference on Wind Effects on Building and Structures, Teddington, London 1963, HMSO.
- [22] **Gatshore, I.S.**, "Two-Dimensional Turbulent Wake," *Journal of Fluid Mechanics*, Vol.30, Part-iii, 1930, p.533.



- [23] **Hayashi, M., Akirasakurai and Yujioha**, "Wake Interference of a Row of Normal Flat Plates Arranged side by side in a Uniform Flow", *Journal of Fluid Mechanics*, Vol. 164, 1986, p. 1-25.
- [24] **Hogg, A.D and Edwards, A.T.**, "Conductor galloping studies in Ontario hydro," 2nd Int. Seminar on wind Effects on Buildings and Structures, Ottawa 1967, University of Toronto Press.
- [25] **Hua, C.K.**, "The behavior of Lift Fluctuations on the Square Cylinders in the Wind Tunnel Test," *Proceedings of the Third International Conference on Wind Effects on Buildings and Structures*, Tokyo, Japan, 1971, p. 911-920.
- [26] **Hussain, H. S. and Islam, O.**, "Study of Wind Load on Buildings and Structures", *Journal of the Institution of Engineers, Bangladesh*, Vol. 1, Nos. 2-3, July-October, 1973.
- [27] **Islam, O.**, Part-I, Possibilities of Wind Effect in Bangladesh, Department of Aeronautical and Mechanical Engineering, University of Salford, UK, July 1976.
- [28] **Islam, T.**, "An Experimental Investigation of Wind Effect on Rectangular Cylinders", M. Sc. Thesis, BUET, Dhaka, 1988.
- [29] **Isyumov, N. and Davenport, A.G.**, "Comparison of full scale and Wind Tunnel Measurements on Commerce Court Plaza," *J. Indust. Aerodynamics*, 1(2), October 1975.
- [30] **Jensen M.**, "Some Lessons Learned in Building Aerodynamics Research," *Proceedings of the Second Conference on Wind Effects on Building and Structures*, Vol. 1, September, 1967.
- [31] **Kelnhofer, J.**, Influence of a Neighboring Building on Flat Roof Loading, *Proceedings of the Third International Conference on Wind Effects on Buildings and Structures*, Tokyo, Japan, 1971, p.221-230.
- [32] **Keffer, J. F.**, "The uniform Distribution of a Turbulent Wake," *Journal of Fluid Mechanics*, Vol. 22, Part-I, 1965, p.135.
- [33] **Koenig, K. and Roshiko, A.**, "An Experimental Study of Geometrical Effects on the Canada, 1967, Vol. II, P.243-282.
- [34] **Lamb, H.**, *Hydrodynamics*, Cambridge University Press, 1932.
- [35] **Lanoville, A., Gatshore, I.S. Parkinson, G.V.**, "An explanation of some effects of turbulence on bluff bodies," *Proceedings of the 4th International Conference on Wind Effects on Buildings and Structures*, London, U.K, 1975, p.333-341.

- [36] **Lawson, T.V.**, "Wind Loading of Buildings, Possibilities from a Wind Tunnel Investigation," University of Bristol, U.K. Report No. TVL/731A, August, 1975.
- [37] **Lee, B.E.**, "The Effect of Turbulence on the surface Pressure Field of a Square Prism", *Journal of Fluid Mechanics*, Vol. 69, 1975, p.263-282.
- [38] **Leutheusser, J.**, "Static Wind Loadings of Grouped Buildings", *Proceedings of the 3rd International Conference on Wind Effects on Buildings*, Tokyo, Japan, 1971, p.211-220.
- [39] **Mandal, A.C.**, "A Study of Wind Effects on Square CYLINDERS", M. Sc. Thesis, BUET, 1979.
- [40] **Maskell, E.C.**, "A Theory of Blockage Effects on Bluff Bodies and Stalled Wings in a Closed Wind Tunnel," ARC R&M No.3400, 1965, HMSO.
- [41] **Matsumoto, M.**, "The Dynamical Forces Acting on the Vibrating Square Prism in a Steady Flow," *Proceedings of the Third International Conference on Wind Effects on Buildings and Structures*, Tokyo, Japan, p.921-930.
- [42] **Mchuri, F.G. Sherratt, A.F.C. and A.S.**, "Effect of the Free Stream Turbulence on Drag Coefficient of Bluff Sharp-Edged Cylinders," *Nature*, Vol.224, No. 5222, November 29, 1969, p.908-909.
- [43] **Melbourne, W.**, "Criteria for Environmental Wind Conditions," *J. Indust. Aerodynamics*, 3(2/3), July 1978.
- [44] **Modi, V.J. and E.L. Sherbiny, S.**, "Wall Confinement Effect on Bluff Bodies in Turbulent Flows, *Proceedings of the Fourth International Conference on Wind Effects on Buildings and Structures*, London, U.K, 1975, p.121-132.
- [45] **Nakamura, Y. and Matsukawa, T.**, "Vortex Excitation of Rectangular Cylinders with a long side normal to the Flow," *Journal of Fluid Mechanics*, Vol.180, 1987,p.171-191.
- [46] **Nakamura, Y. and Ohya, Y.**, "The Effects of Turbulence on the Main Flow Past Square Rods," *Journal of Fluid Mechanics*, Vol.137, 1983, p.331-345.
- [47] **Nakamura, Y. and Yujioha.**, "Vortex shedding from Square Prisms in Smooth and Turbulent Flows," *Journal of Fluid Mechanics*, Vol.164, 1986, p.77-89.
- [48] **Okajima, A.**, "Strouhal Numbers of Rectangular Cylinders," *Journal of Fluid Mechanics*, Vol. 123, 1982, p.379-398.

- [49] **Parkinson, G.V. and Modi, V.J.**, "Recent Research on Wind Effects on Bluff Two Dimensional Bodies," Proceedings, International Research Seminar, Wind Effects on Buildings and Structures, Ottawa, Canada, 1967, p.485-514.
- [50] **Pearlstein, A.J. W.J. Mantle.**, National Science Foundation CTS 94-22770, "Stability and the Transition to Three-Dimensional in Flows Past Axisymmetric Bluff Bodies," The Summary of Engineering Research-2000, College of Engineering, University of Illinois at Urbana-Champaign, USA.
- [51] **Pearlstein, A.J. F. Pettani, L. Wang.**, "Stability of the Wake Behind a Rotating Circular Cylinder," The Summary of Engineering Research-2000, University of Illinois, USA.
- [52] **Peris, R. Action Du Vont Sur Les cheminees De Grand Hantour.**, Proceedings, International Research Seminar, Wind Effects on Buildings and Structures, Ottawa, Canada, 1967, Vol. II, p.243-282.
- [53] **Pope, A. and Harper, J.J.**, "Low Speed Wind Tunnel testing", John Willy and Sons, New York, 1996.
- [54] **Roberson, J.A. Chi Yu Lin. Rutherford G.S. and Stine M.D.**, "Turbulence Effects on Drag of Sharp-edged Bodies," Journal of Hydraulics Division, Vol. 98, No. HY7, p.1187-1201.
- [55] **Roberson, J.A. Crowe, C.T., Tseng, R.**, "Pressure Distribution on Two and Three Dimensional Models at Small Angles of Attack in Turbulent Flow", Proceedings of the 2nd U.S. National Conference on Wind Engineering Research, June 22-25, Colorado, 1975.
- [56] **Robertson, J.M.**, "Pressure field at Reattachment of separated Flows", Proceedings of the 2nd U.S National Conference on Wind Engineering Research, June 22-25, 1975, Colorado.
- [57] **Roy, U.K. Seraj S.M.**, BUET, Bangladesh and RLP Hodgson, University of Exeter, UK, "Pressure Distribution Characteristics on a Typical Bangladeshi Rural Home", J. Institution of Engineers, Bangladesh, Multidisciplinary Vol. Mul-dis. 25, No. 1, December 2000, P-62-67.
- [58] **Sakamoto, H. and Arie, M.**, "Vortex Shedding from a Rectangular Prism and a Circular Cylinder Placed Vertically in Turbulent Boundary Layer," Journal of Fluid Mechanics, Vol. 126, 1983, p.147-165.

- [59] **Scruton, C. and Rogers E.M.E.**, "Steady and unsteady wind loading of Buildings and Structures," Proceedings R.Soc. A, 269, 1971, 353-85.
- [60] **Surry, D.**, "Pressure Measurements on the Texas Tech Building: Wind Tunnel Measurements and Comparison with Full Scale, J. Wind Eng. Ind. Aerodynamics. no.38, 1991, p.235-247.
- [61] **Vickery, B.J.**, "Fluctuating Lift and Drag on a Long Cylinder of Square Cross Section in a Smooth and in a turbulent Stream," Journal of Fluid Mechanics, Vol.25, 1966, p.481-491.
- [62] **Whitbread, R. E.**, Model simulation of Wind Effects on Structures, "Proceedings of a symposium on Wind Effects on Buildings and Structures", Teddington, UK, 1963, P. 283-301.

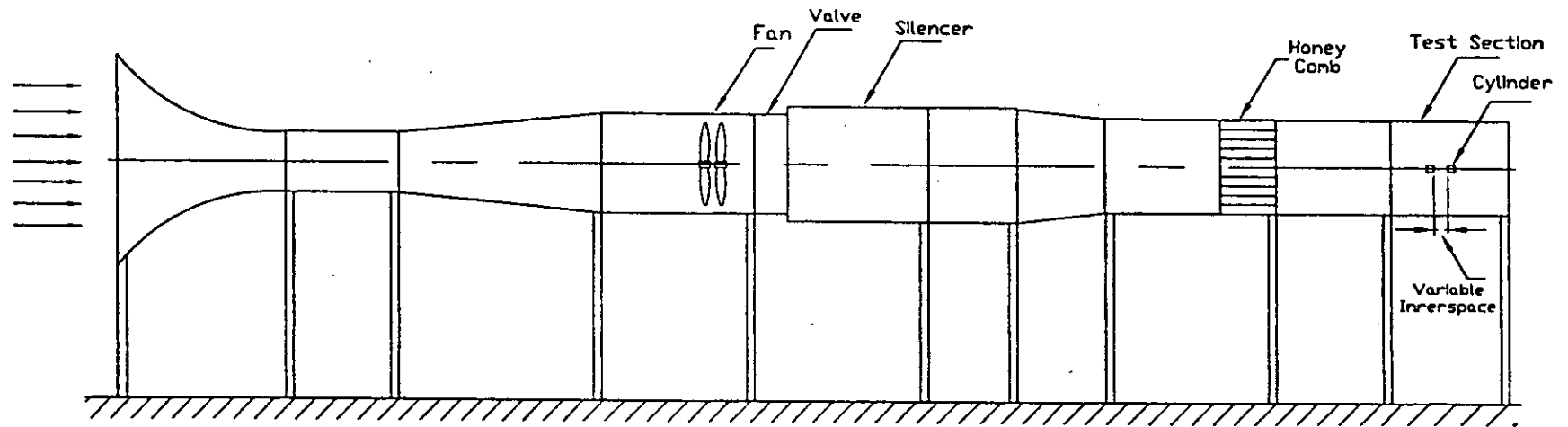
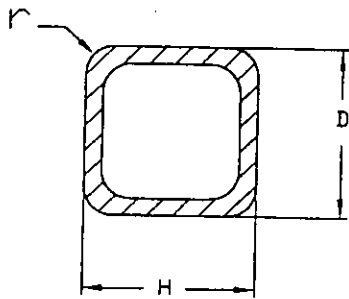
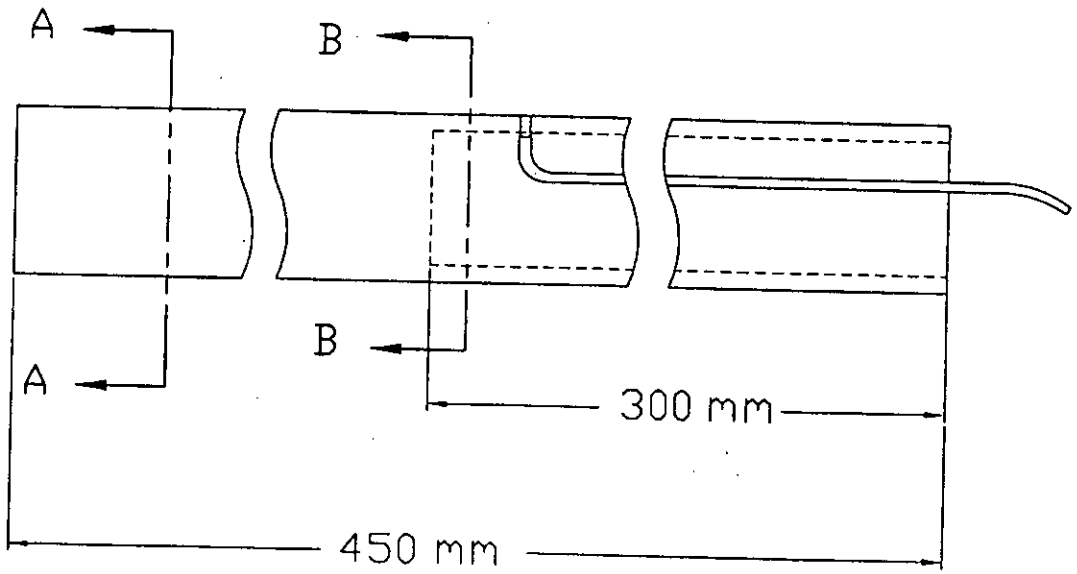
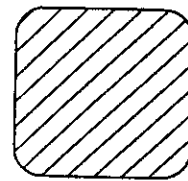


Figure 3.1: Schematic Diagram of the Wind Tunnel

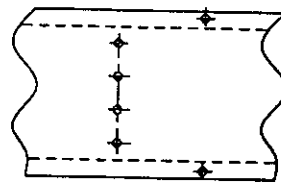
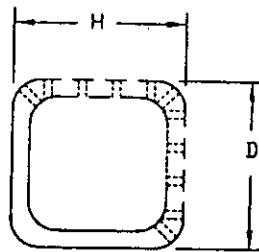


B-B Section



A-A Section

(a)



(b)

Figure 3.2: Constructional Details of Cylinder

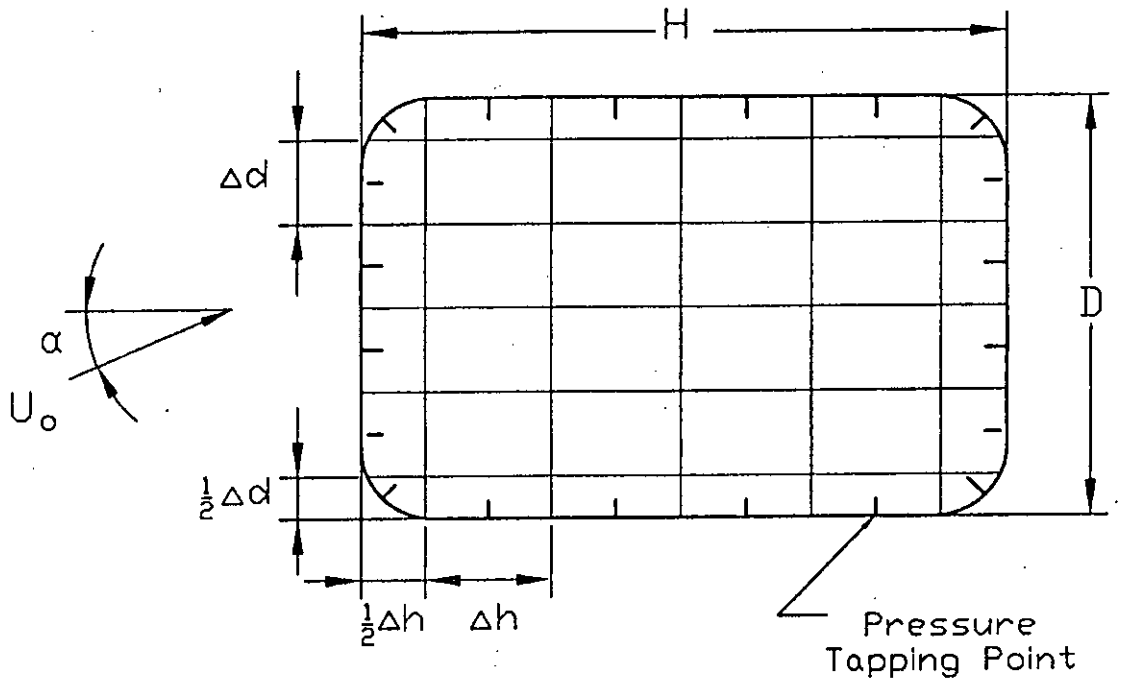


Figure 4.1: Section of a Cylinder Showing Pressure Tapping Position

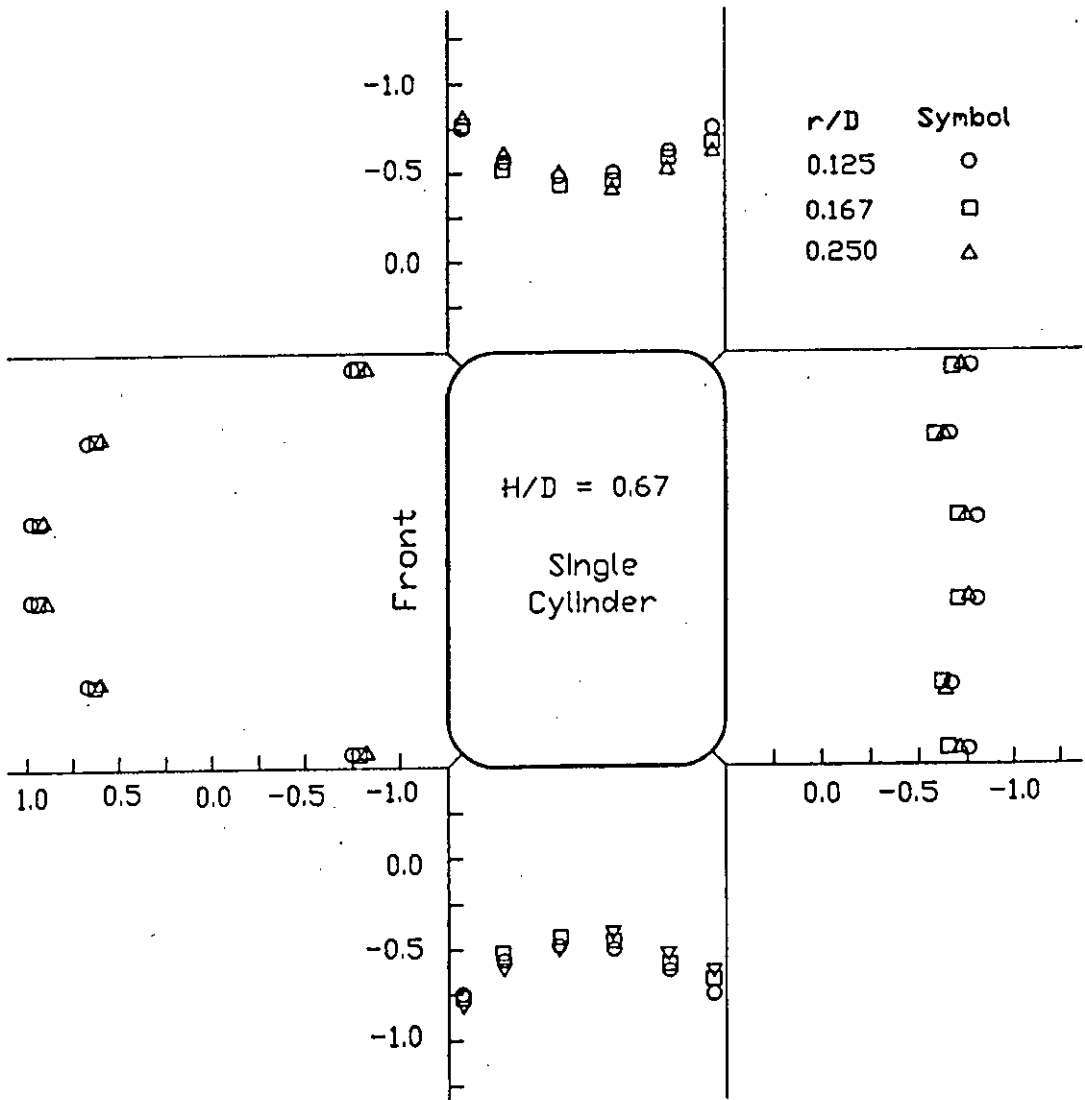


Figure 5.1: Distribution of Static Pressure Coefficient on Single Cylinder with Side Ratio (H/D) of 0.67 at Various Nose Radius (r/D)



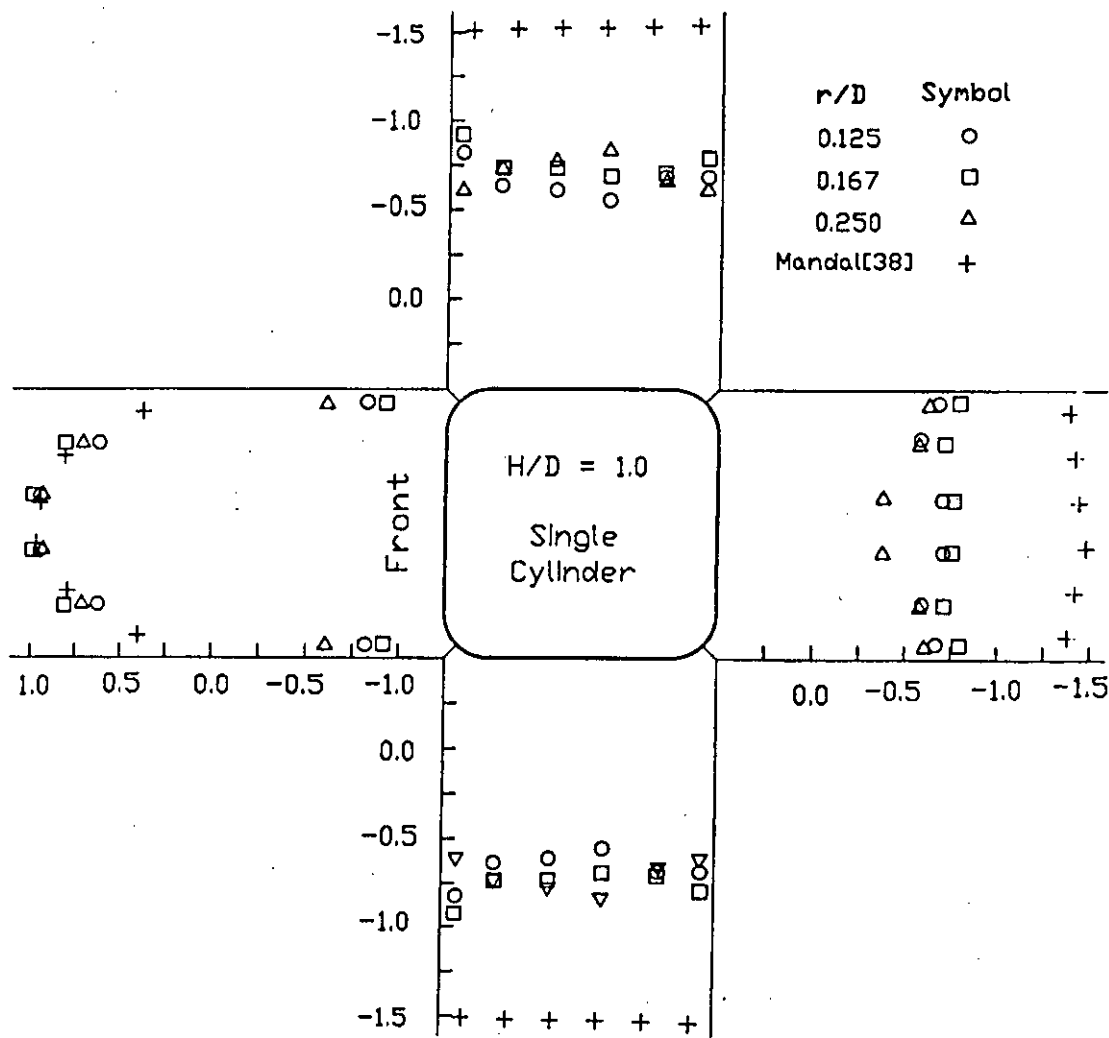


Figure 5.2: Distribution of Static Pressure Coefficient on Single Cylinder with Side Ratio (H/D) of 1.0 at Various Nose Radius (r/D)

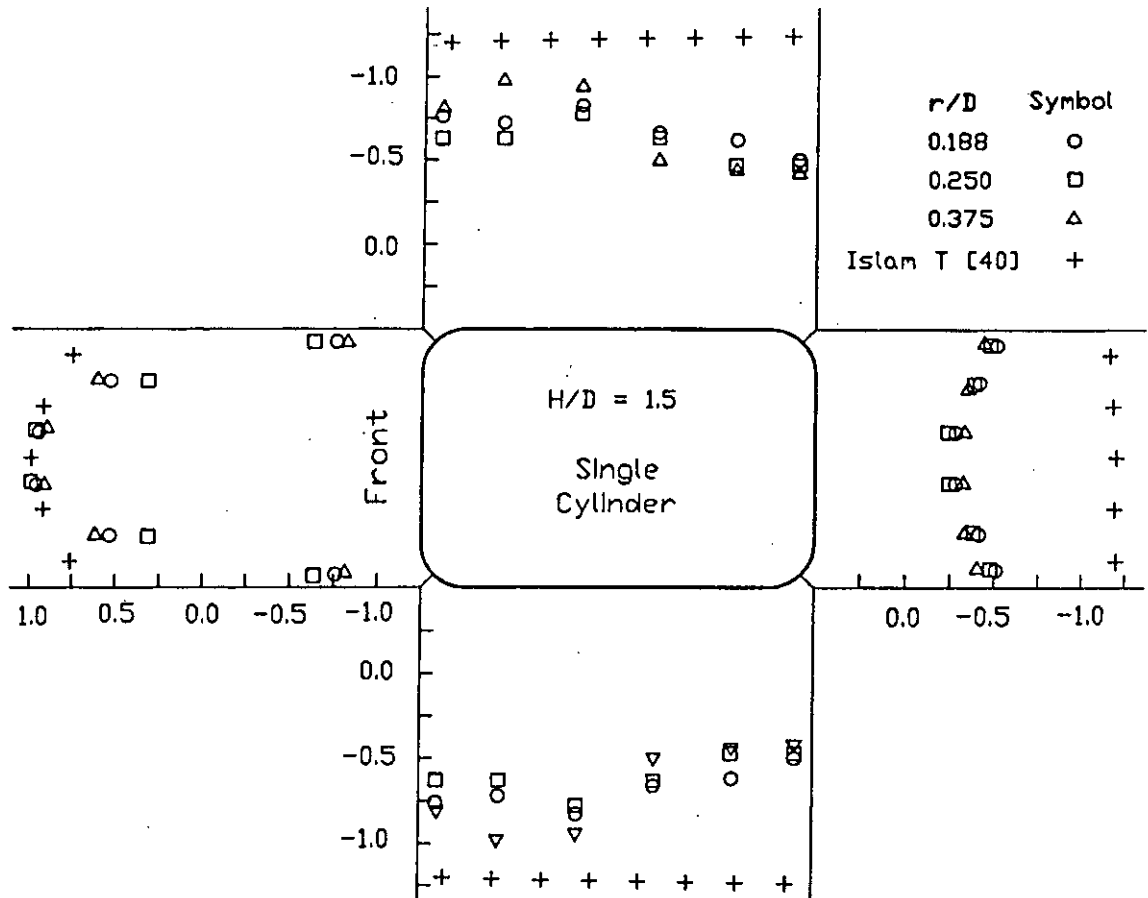
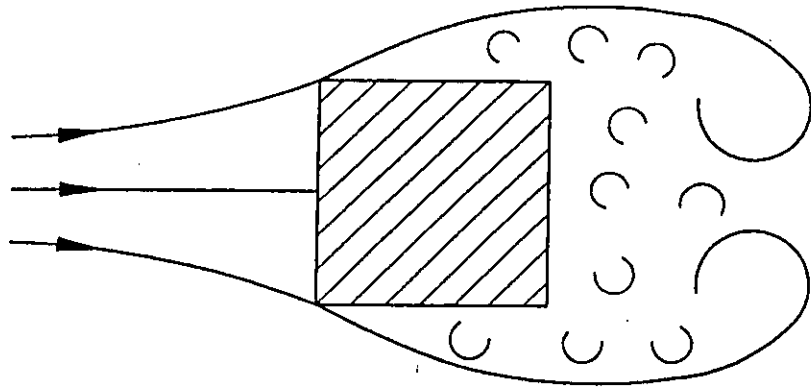
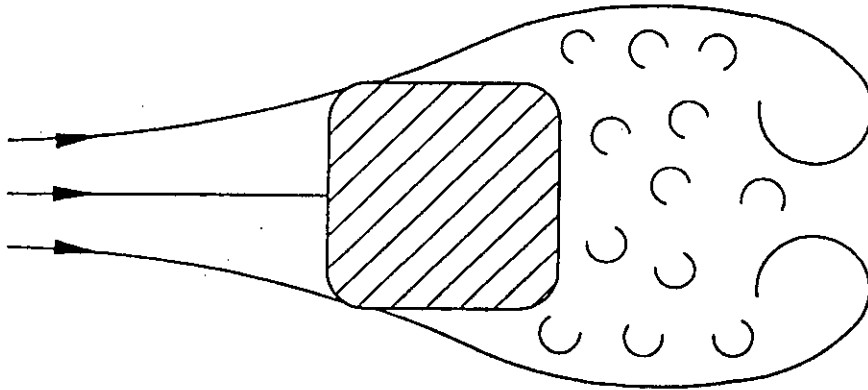


Figure 5.3: Distribution of Static Pressure Coefficient on Single Cylinder with Side Ratio ( $H/D$ ) of 1.5 at Various Nose Radius ( $r/D$ )



(a)



(b)

Figure 5.4: Typical Nature of Flow Characteristics For a Sharp Edged and Rounded Edged Cylinders

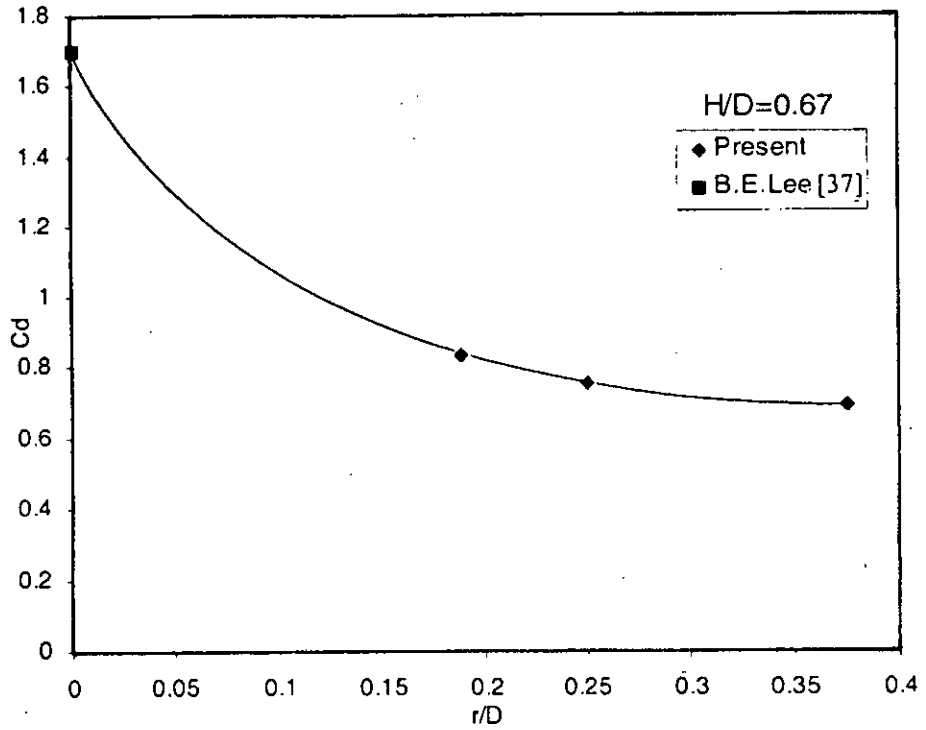


Figure 5.5: Variation of Drag Coefficient with Nose Radius ( $r/D$ ) at Side Ratio ( $H/D$ ) of 0.67 for Single Cylinder

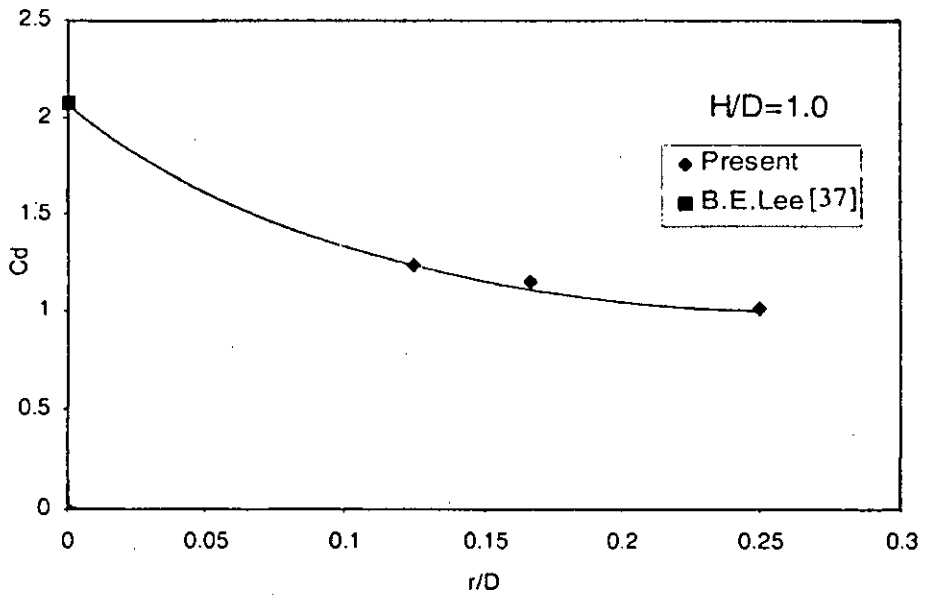


Figure 5.6: Variation of Drag Coefficient with Nose Radius ( $r/D$ ) at Side Ratio ( $H/D$ ) of 1.0 for Single Cylinder

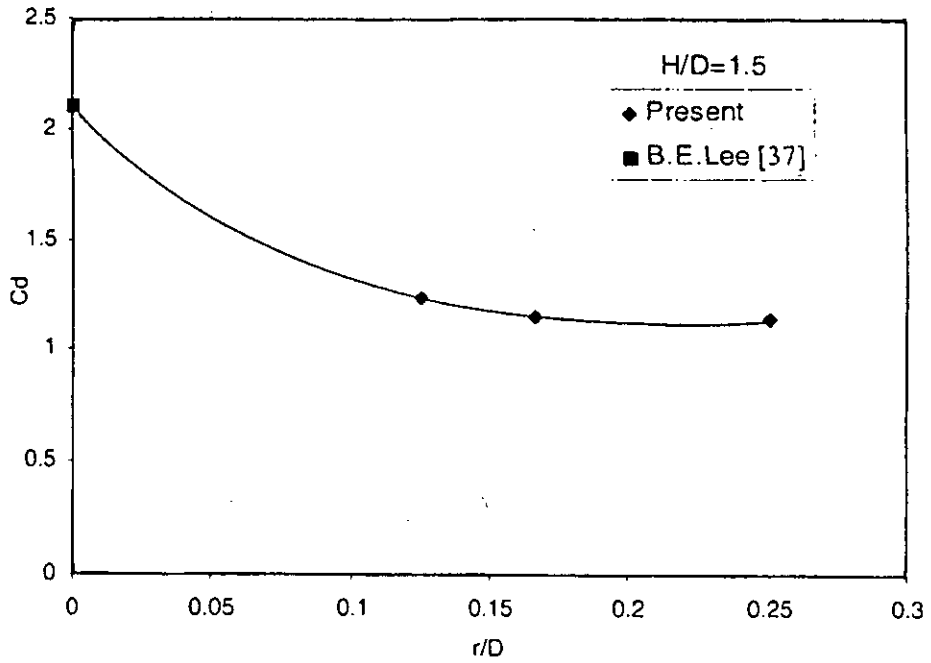


Figure 5.7: Variation of Drag Coefficient with Nose Radius ( $r/D$ ) at Side Ratio ( $H/D$ ) of 1.5 for Single Cylinder

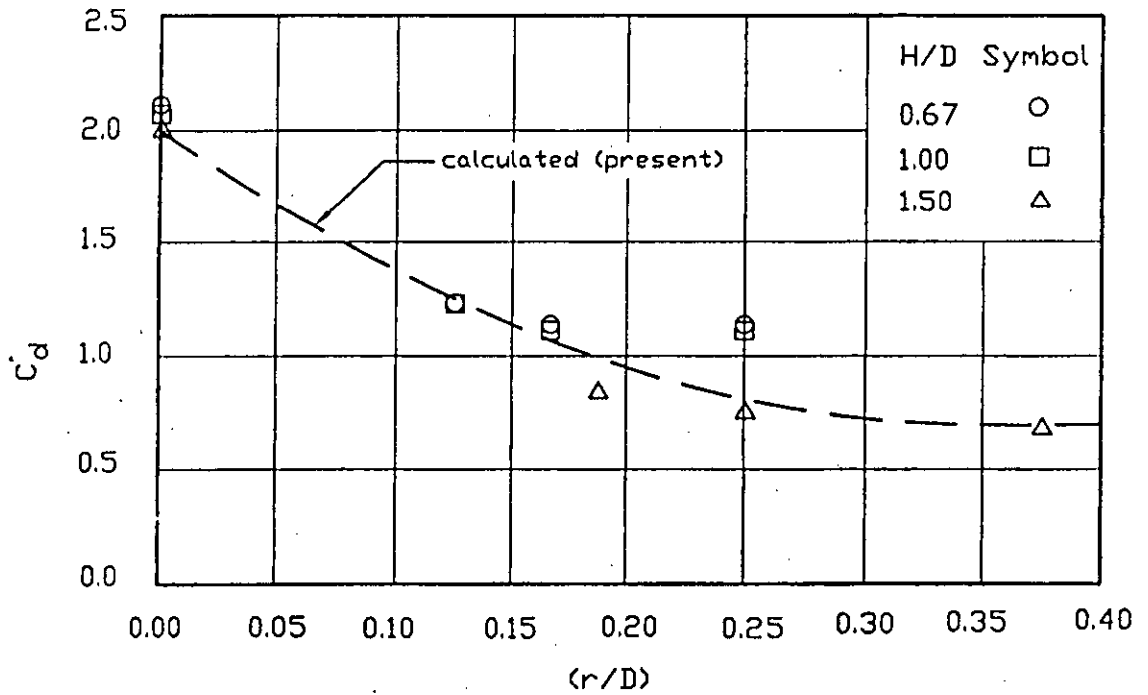


Figure 5.8: Comparison of Drag Coefficient ( $C_d$ ) for various side ratios ( $H/D$ ) on Single Cylinder

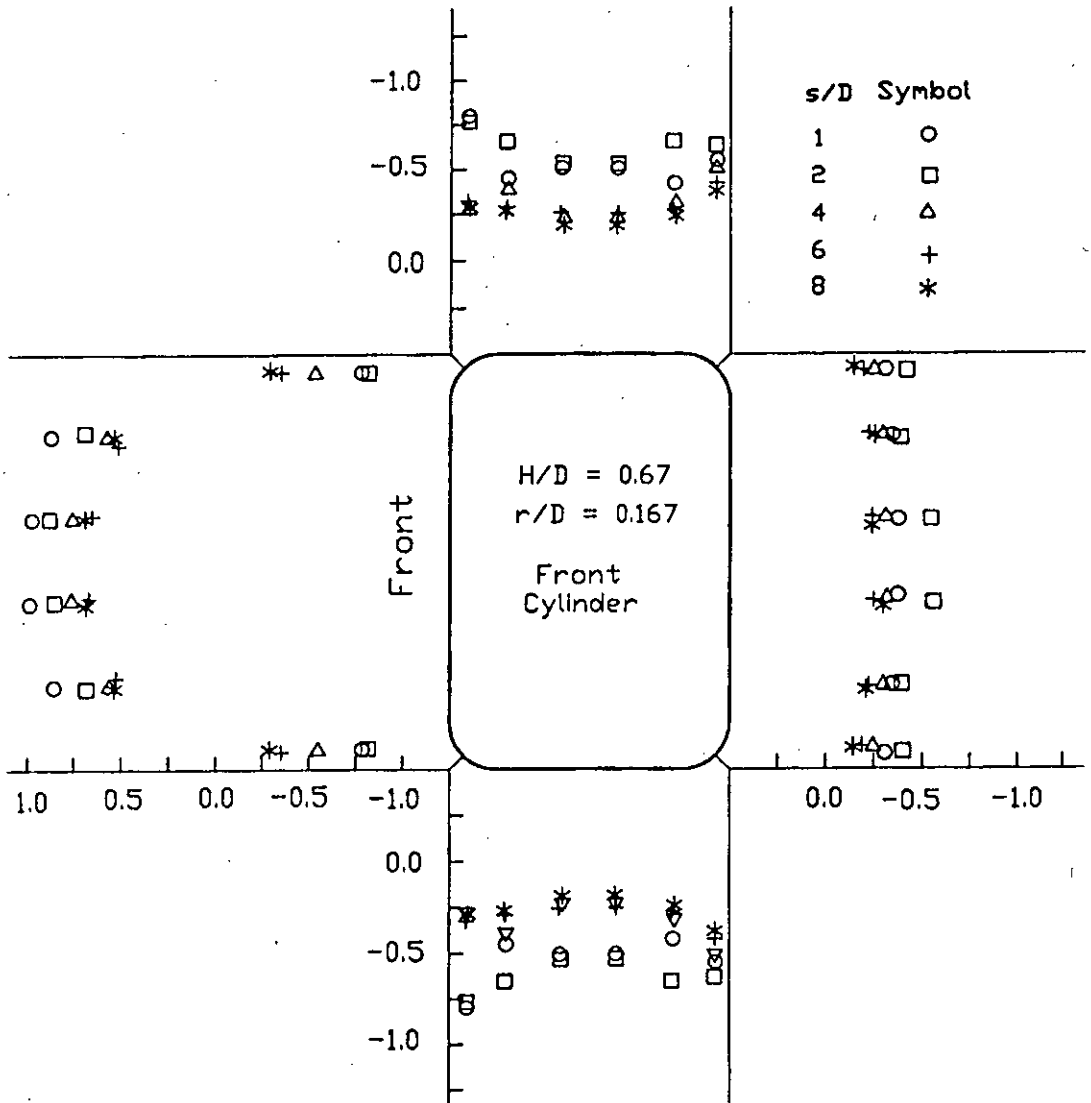


Figure 5.9: Static Pressure Distribution on Front Cylinder in a Group with Side Ratio (H/D) of 0.67 and Nose radius (r/D) of 0.167 for Various Interspace (s/D)

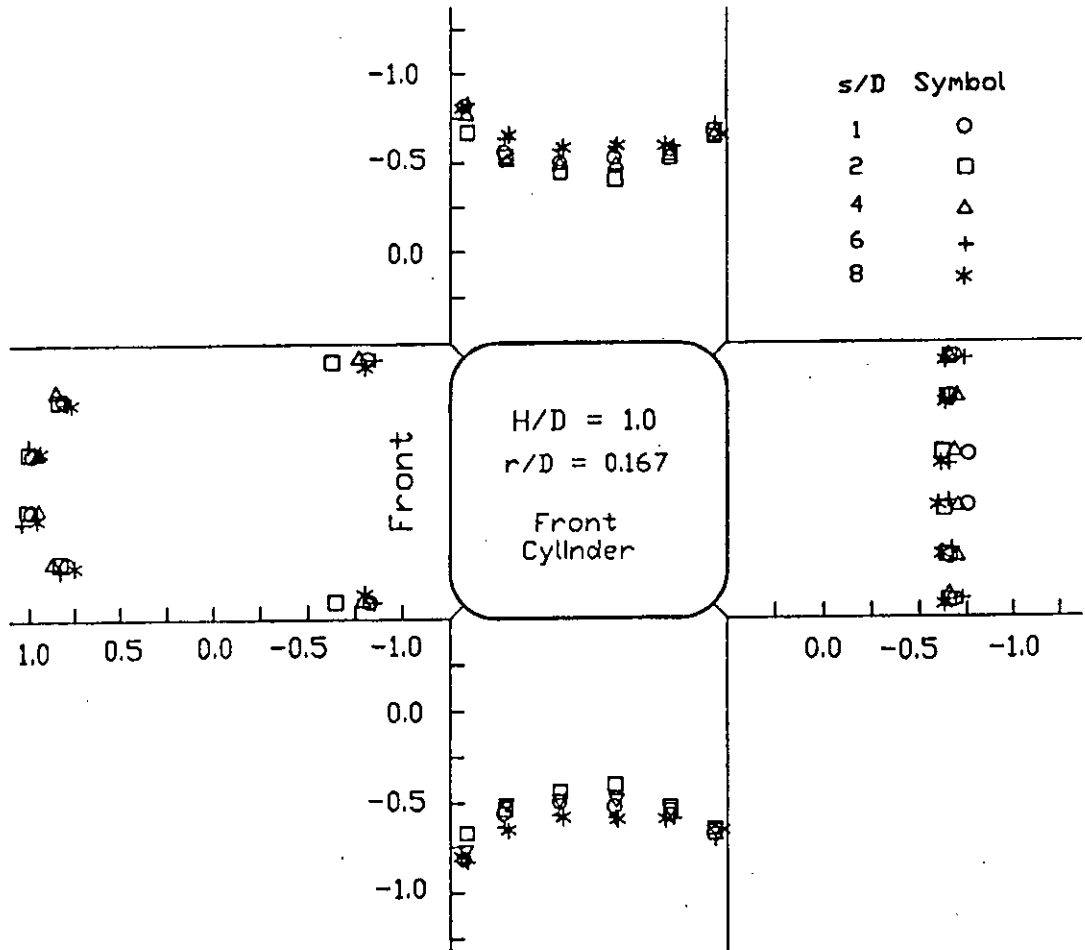


Figure 5.10: Static Pressure Distribution on Front Cylinder in a Group with Side Ratio ( $H/D$ ) of 1.0 and Nose radius ( $r/D$ ) of 0.167 for Various Interspace ( $s/D$ )

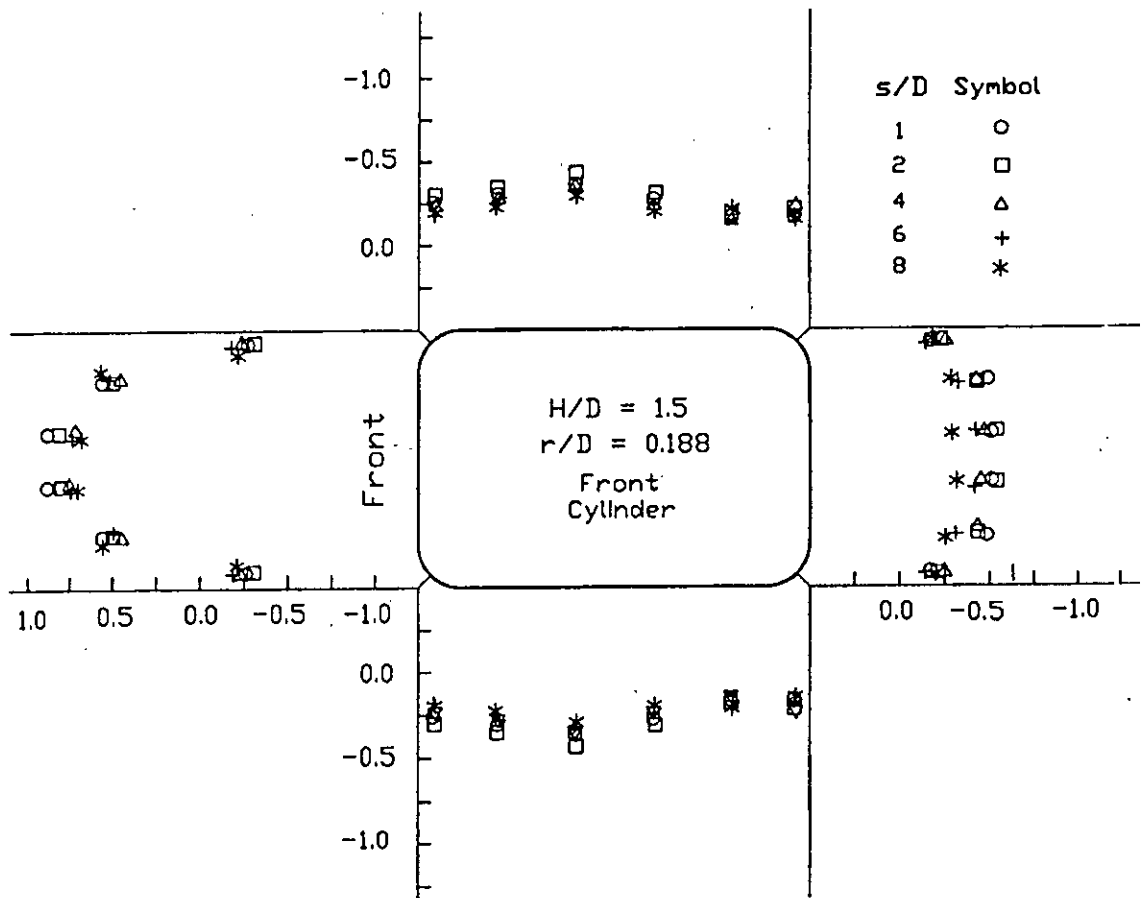


Figure 5.11: Static Pressure Distribution on Front Cylinder in a Group with Side Ratio ( $H/D$ ) of 1.5 and Nose radius ( $r/D$ ) of 0.188 for Various Interspace ( $s/D$ )



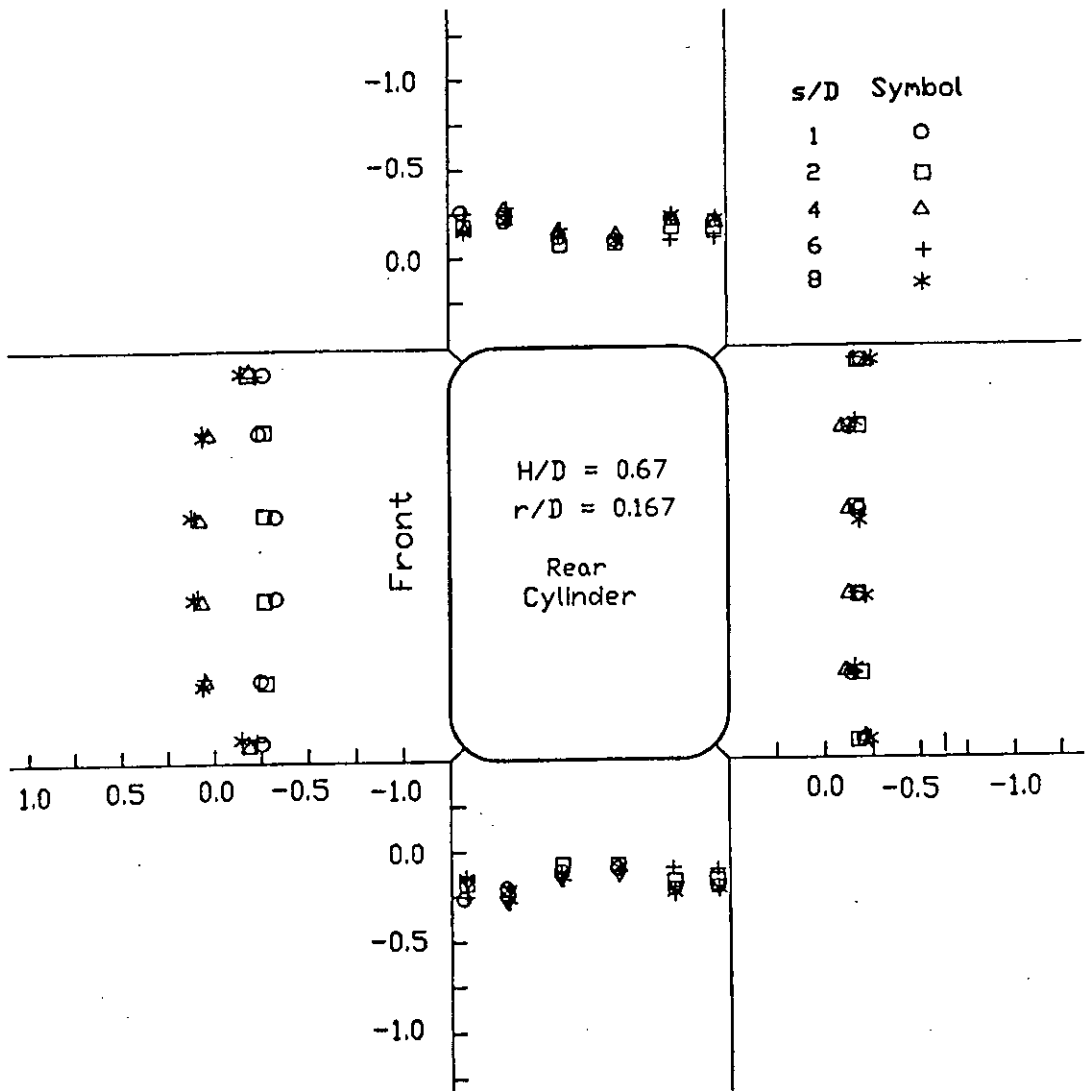


Figure 5.12: Static Pressure Distribution on Rear Cylinder in a Group with Side Ratio ( $H/D$ ) of 0.67 and Nose radius ( $r/D$ ) of 0.167 for Various Interspace ( $s/D$ )

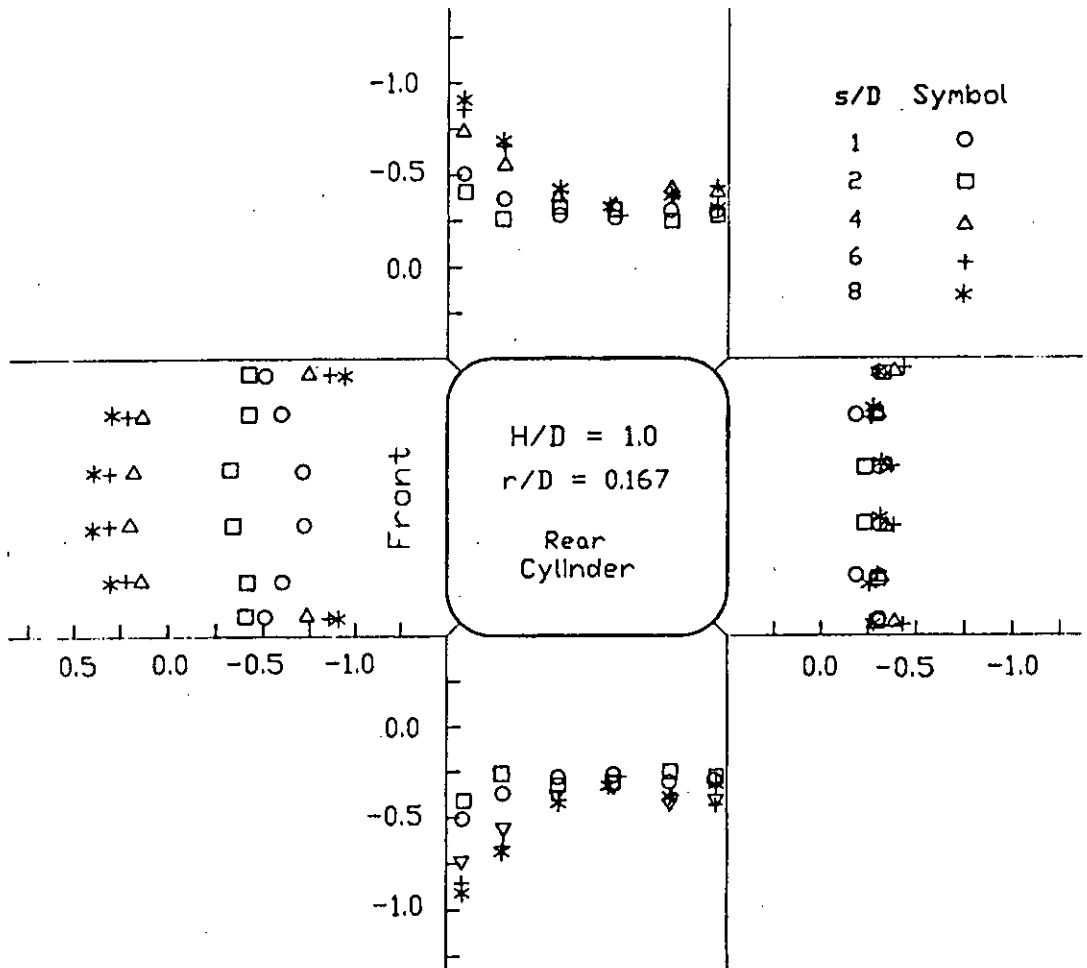


Figure 5.13: Static Pressure Distribution on Rear Cylinder in a Group with Side Ratio (H/D) of 1.0 and Nose radius (r/D) of 0.167 for Various Interspace (s/D)

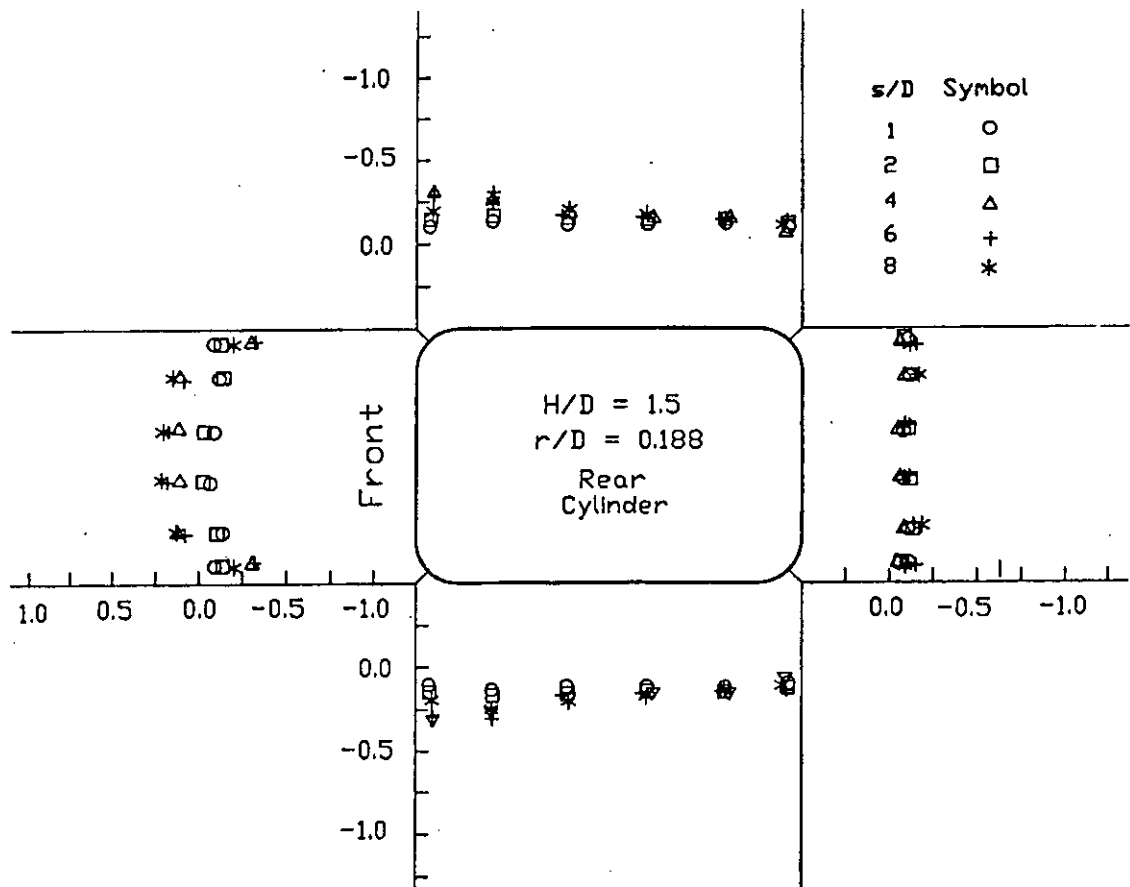


Figure 5.14: Static Pressure Distribution on Rear Cylinder in a Group with Side Ratio ( $H/D$ ) of 1.5 and Nose radius ( $r/D$ ) of 0.188 for Various Interspace ( $s/D$ )

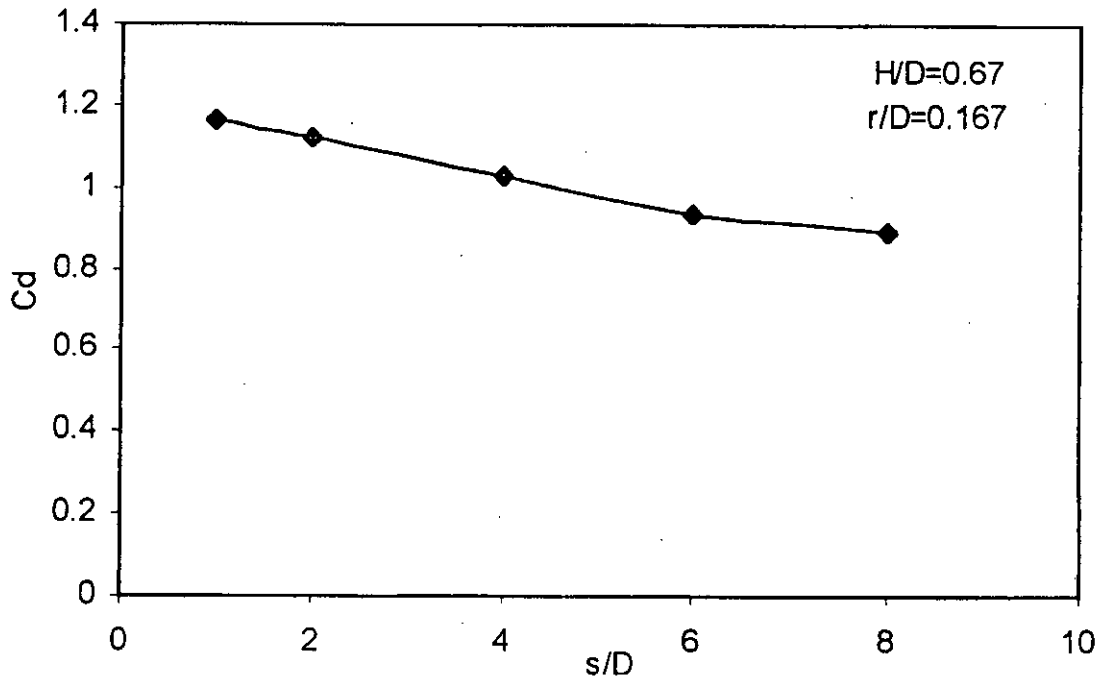


Figure 5.15: Variation of Drag Coefficient ( $C_d$ ) with Interspace ( $s/D$ ) on Front Cylinder with Side Ratio ( $H/D$ ) of 0.67 at Nose Radius ( $r/D$ ) of 0.167

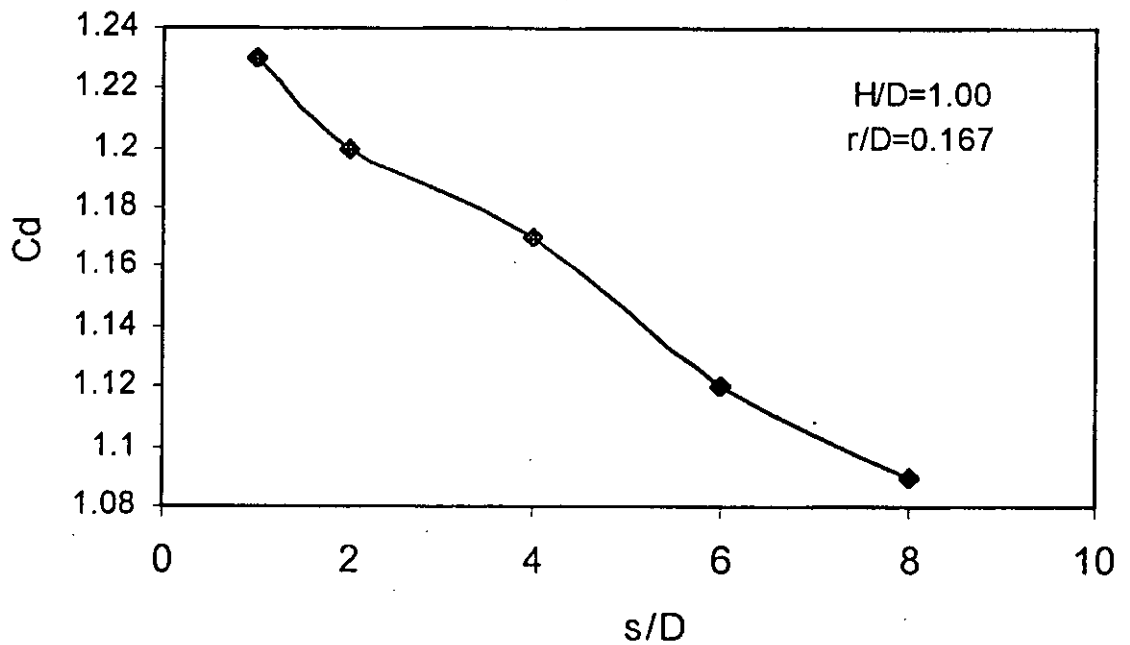


Figure 5.16: Variation of Drag Coefficient ( $C_d$ ) with Interspace ( $s/D$ ) on Front Cylinder with Side Ratio ( $H/D$ ) of 1.0 at Nose Radius ( $r/D$ ) of 0.167

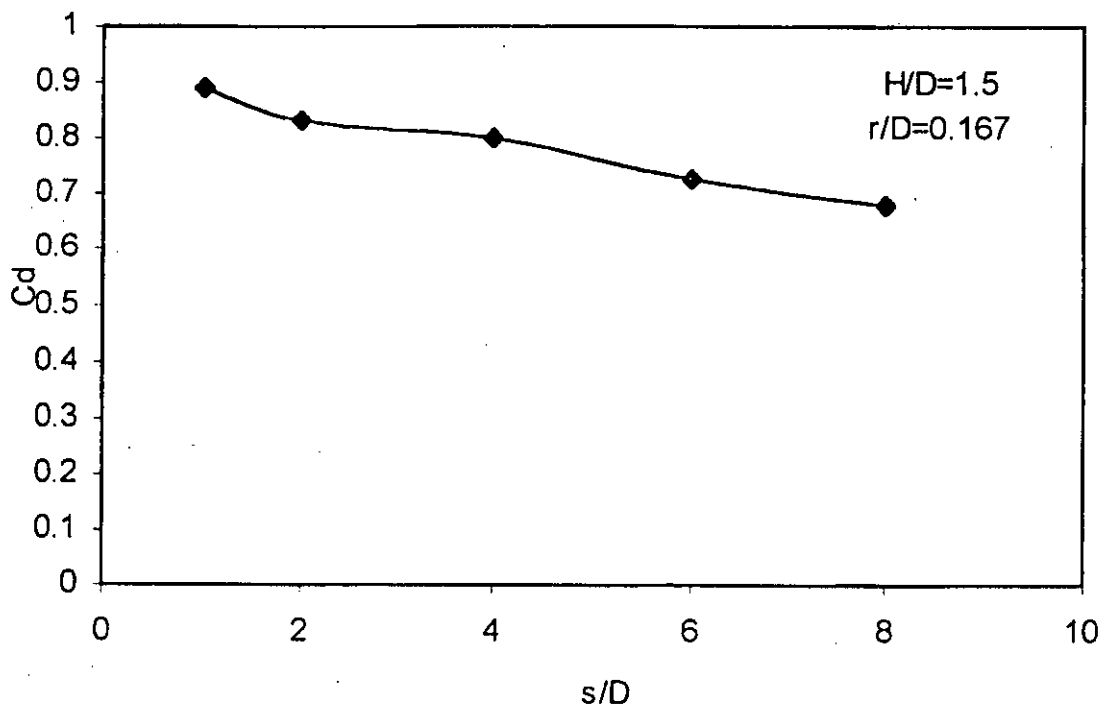


Figure 5.17: Variation of Drag Coefficient ( $C_d$ ) with Interspace ( $s/D$ ) on Front Cylinder with Side Ratio ( $H/D$ ) of 1.5 at Nose Radius ( $r/D$ ) of 0.167

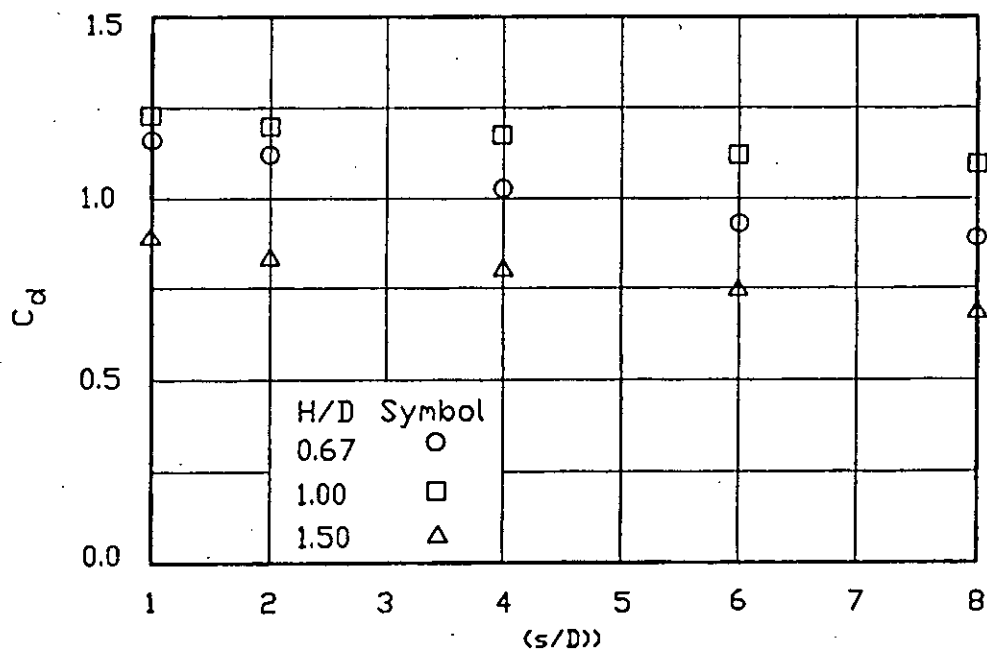


Figure 5.18: Comparison of Drag Coefficient at Various Side Ratio ( $H/D$ ) on Front Cylinder

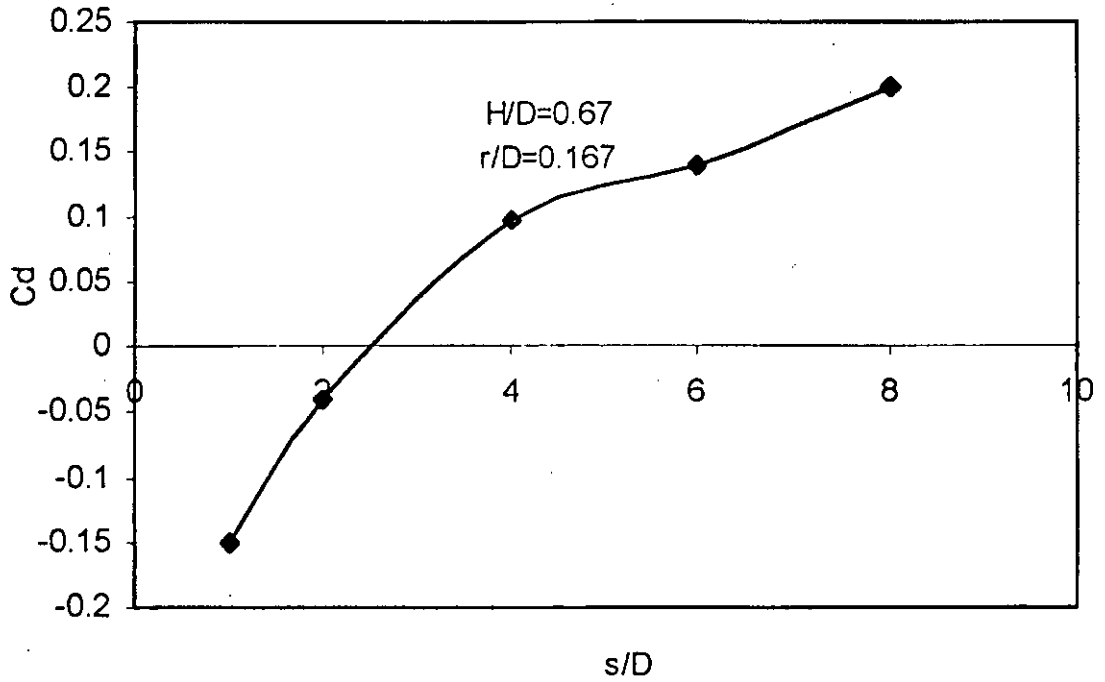


Figure 5.19: Variation of Drag Coefficient ( $C_d$ ) with Interspace ( $s/D$ ) on Rear Cylinder with Side Ratio ( $H/D$ ) of 0.67 at Nose Radius ( $r/D$ ) of 0.167

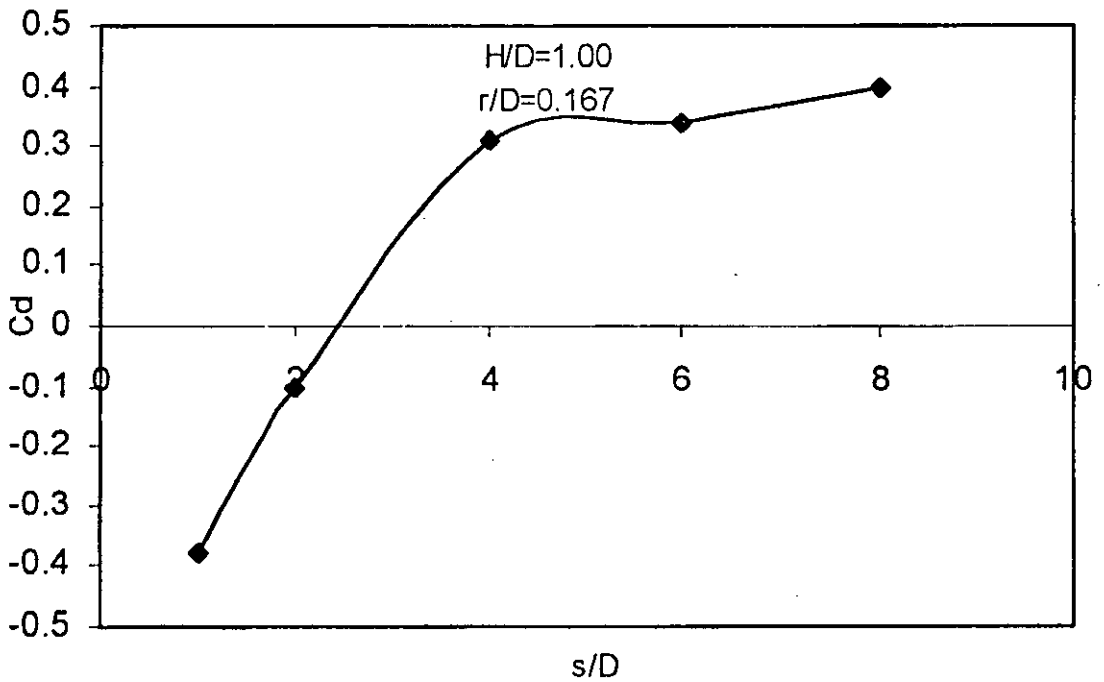


Figure 5.20: Variation of Drag Coefficient ( $C_d$ ) with Interspace ( $s/D$ ) on Rear Cylinder with Side Ratio ( $H/D$ ) of 1.0 at Nose Radius ( $r/D$ ) of 0.167

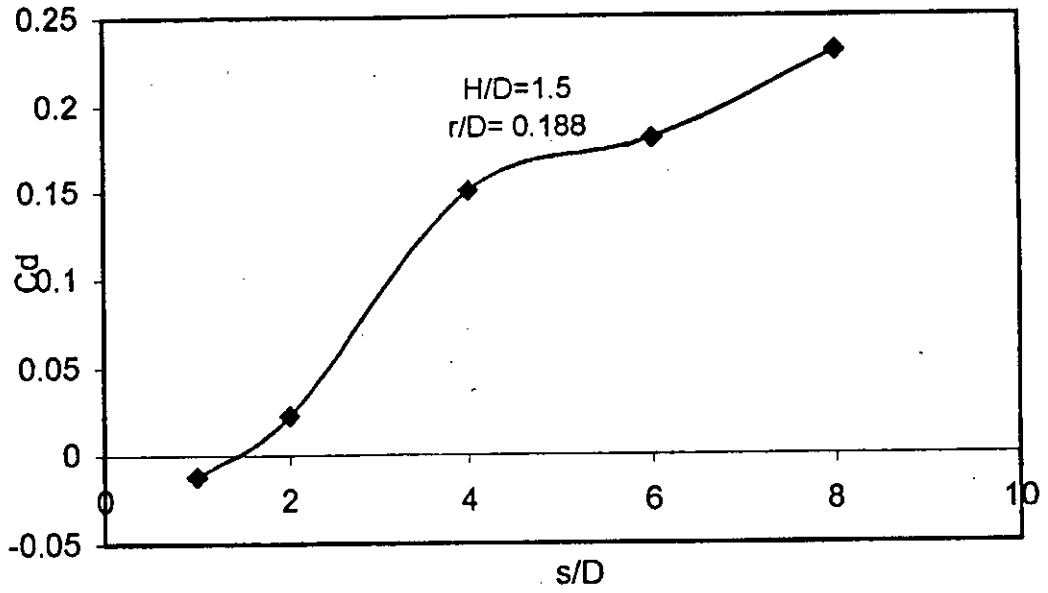


Figure 5.21: Variation of Drag Coefficient ( $C_d$ ) with Interspace ( $s/D$ ) on Rear Cylinder with Side Ratio ( $H/D$ ) of 1.5 at Nose Radius ( $r/D$ ) of 0.188

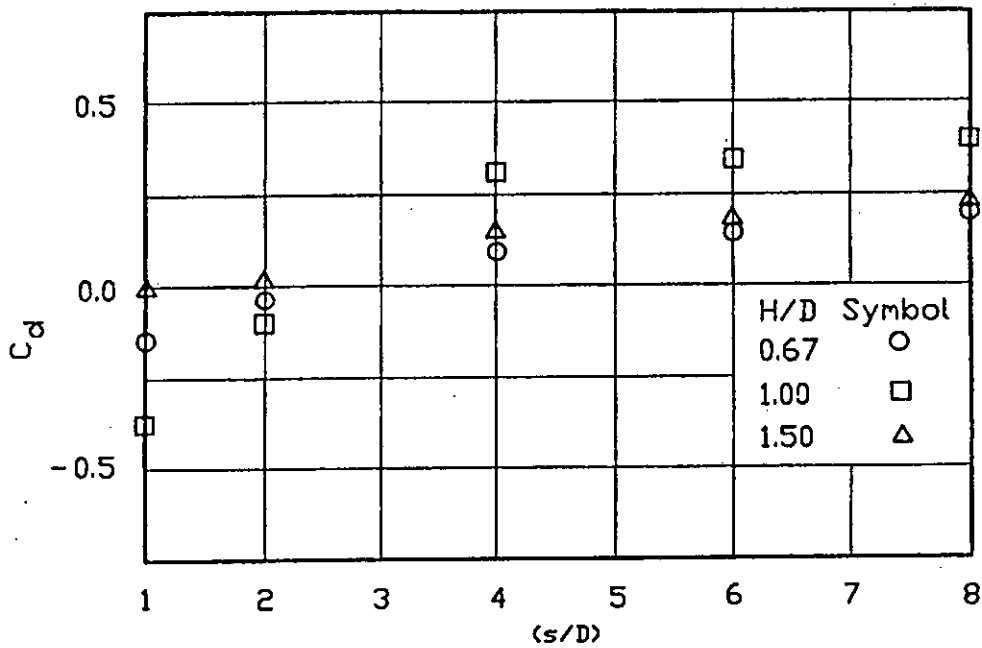


Figure 5.22: Comparison of Drag Coefficient ( $C_d$ ) on Rear Cylinder with Interspace ( $s/D$ ) at Various Side Ratios ( $H/D$ )

